Petrogenesis of calc-alkaline andesite from Rishiri volcano, northern Hokkaido

*Hajime Taniuchi[1], Takeshi Kuritani[2], Mitsuhiro Nakagawa[2]

1. Department of Natural History Science, Graduate School of Science, Hokkaido University, 2. Department of Natural History Science, Fuculty of Science, Hokkaido University

1. Introduction

Volcanic rocks can provide useful information on the growth of the crust and the temporary change of the composition and thermal structure of the mantle beneath the volcano. Rishiri volcano is located in northern Hokkaido where no other active volcano is present. Therefore, it is a suitable target to elucidate the petrological evolution of a single volcano (Ishizuka and Nakagawa, 1999). Calc-alkaline andesite is a typical rock series in many island arcs and the composition is similar to the average composition of the continental crust. In Rishiri volcano, calc-alkaline andesite is a dominant rock type during a climactic volcanic stage. To understand the petrological evolution of the volcano, it is necessary to clarify the magmatic process of the calc-alkaline andesite. In this study, we have performed petrological and geochemical analysis of calc-alkaline andesite to understand the magmatic process.

2. Petrology

Whole-rock SiO_2 content of the products ranges from 58.2 wt.% to 65.3 wt.%, and they are divided into A-type (Andesite-type; SiO_2<62.5 wt.%) and D-type (Dacite-type; SiO_2>63.9 wt.%). The phenocryst assemblage of the A-type is olivine + cpx + opx + pl, and that of the D-type is cpx + opx + pl. A-type has crystal clots composed of pl ±olivine ±cpx ±opx, gabbroic xenolith and mafic inclusions. Olivine phenocrysts are anhedral and they have reaction rim of orthopyroxene. The Mg-number of the olivine core shows wide range (64-88). Clinopyroxene and orthopyroxene phenocrysts occur in all samples. Pyroxenes phenocrysts in A-type are reversely or normally zoned with wide core compositions. In contrast, pyroxenes phenocrysts in D-type only show normal zonation with narrow core composition. Plagioclase phenocryst are found in all samples. An-content of the plagioclase core in A-type (45-88) is wider than in D-type (49-59). Major and trace elements concentrations show linear trends in Harker diagrams except for Cr, Ni, Sr, Ba and Zr. Eu anomaly is found only in A-type. With increasing the SiO_2 contents, the $^{87}Sr/^{86}Sr$ and $^{206}Pb/^{204}Pb$ ratios tend to increase. The $^{143}Nd/^{144}Nd$ ratios of A-type is higher than those of D-type. There is no significant difference of the estimated P-T condition of the magma chamber between A-type(P=3.6-4.1 kbar, T=970-1000℃) and D-type(P=4.1 kbar, T=970-980℃)(two-pyroxene geo-thermometer and barometer; Putirka, 2008).

3. Discussion

The Petrological features suggest that the calc-alkaline andesite was produced by magma mixing between mafic and felsic magma. The basaltic endmember magma is suggested to have been heterogeneous on the basis of the observations that 1)the compositional trends of Ni and Cr are not linear in Harker diagram, 2)modal abundance of olivine phenocryst is the highest at around SiO_2=60 wt.%, 3)wide core composition of olivine and plagioclase. In contrast, there is no petrological evidence for magma mixing in D-type, so we interpret that D-type represents the felsic endmember magma. Therefore, A-type magma was produced by magma mixing between D-type (felsic endmember) magma and the heterogeneous basaltic endmember magma.

The chemical and isotopic composition of D-type (felsic endmember) are similar to those of high-SiO2 Adakite (Martin, 2005) and they have significantly high-MgO, Cr and Ni concentration. This adakitic composition cannot be derived from any alkaline basalts at Rishiri volcano by crystallization and differentiation process. It is also difficult to explain the adakitic signature by direct melting of the crust,

because the isotopic composition of granodiorite (Kuritani et al., 2005) and gabbroic samples (included in A-type as xenolith) have significantry higher and lower $^{206}Pb/^{204}Pb$ ratios, respectively, than those of D-type samples. Therefore, the possible petrogenesis of the D-type magma is 1)the multiple processes including partial melting, differentiation and assimilation in crustal level, 2)the partial melting of middle crust and 3)the partial melting of the subducted slab.

Keywords: Calc-alkaline andesite, Magma mixing, Adakite, Rishiri Volcano

Genesis of ultra-high-Ni Ol in high-Mg andesite lava triggered by seamount subduction in the northeast Kamchatka

*Tatsuji Nishizawa[1], Hitomi Nakamura[1,2,3], Tatiana Churikova[4], Boris Gordeychik[5], Osamu Ishizuka[6], Qing Chang[2], Atsushi Nakao[1], Hikaru Iwamori[1,2]

1. Department of Earth and Planetary Sciences, Tokyo Institute of Technology, 2. Depertment of Solid Earth Geochemistry, Japan Agency for Marine-Earth Science and Technology, 3. Chiba Institute of Technology, ORCeNG, 4. Institute of Volcanology and Seismology, FED, RAS, 5. Institute of Experimental Mineralogy, RAS, 6. Institute of Geoscience and Geoinfomation, Geological Survery of Japan, AIST

The northeast Kamchatka has undergone extremely dynamic processes, such as (1) hot asthenospheric injection around the slab edge (Yogodzinski et al., 2001), and (2) subduction of the Emperor Seamount Chain (Davaille and Lees, 2004). These processes are considered to be affecting the most active volcanism in the world (Klyuchevskoy Volcanic Group) (Dorendorf et al., 2000) and the northward shallowing of the subduction dip angle (Gorbatov et al., 1997). A monogenetic volcanic East Cone, EC (Fedorenko, 1969) is located in the forearc area ~60 km above the subducting Pacific Plate, which is supposed to be old and cold (~100 Ma, Renkin and Sclater, 1988). In this case, an volcanic zone other than forearc magmatism is expected to be formed above the slab of 100 km depth (Iwamori, 1998) induced by slab-derived fluid and the corresponding mantle melting. We found that the EC lavas exhibit primitive characteristics and show variability in rock-type including high-Mg andesite (HMA) and relatively primitive basalts in time (0.73–0.12 Ma) and (30 km x 60 km area). Olivine phenocrysts in the EC lavas also show different characteristics in each rock-type. Ultra-high-Ni olivine (Ni ~6300 ppm) was observed in HMA, which contain ~6300 ppm Ni, the highest value recorded in arc lavas to date (e.g., Straub et al., 2008). On the other hand the primitive basalt includes moderately-high-Ni olivine (Ni ~2900 ppm). These features reflect the dynamic processes in the northeast Kamchatka.
We discussed the enigmatic forearc magmatism based on the genetic conditions of the HMA, primitive basalt, ultra-high-Ni olivine, and temporal engagement of the seamount subduction. Inversion for trace element compositions involving subducting slab, slab-derived fluid, DMM-type mantle and melt, together with detailed inspection of the assemblages, compositions and zoning profiles of phenocrysts, indicate several isolated melt pockets and/or veins formed at the initial stage of crystallization in the mantle, each being derived from different degrees of pyroxenization along fluid pathways. Silica-rich fluids derived from a subducted seamount expelled beneath the forearc area and its chemical characteristics. Melting of heterogeneously veined mantle with such fluids produced the various primary melts in limited time and space.

Keywords: high-Mg andesite, high-Ni olivine, seamount subduction

Rotational deformation of a rhyolite lava flow below the Curie temperature of magnetite: Sanukayama rhyolite lava in Kozushima Island, Japan

*Kotaro Nakai[1], Kuniyuki Furukawa[2], Tatsuo Kanamaru[3], Koji Uno[1]

1. Graduate School of Education, Okayama University, 2. Faculty of Business Administration, Aichi University, 3. Department of Geosystem Sciences, College of Humanities and Sciences, Nihon University

Rhyolite lava flow often has a total thickness more than one hundred meters, which is made up mainly of grassy part (e.g. Manley and Fink, 1987; Furukawa and Kamata, 2005). A crystal-poor rhyolitic lava shows its flow front advance that lasts long time after the cessation of lava supply (Tuffen et al., 2013). Consolidated upper grassy part can passively be deformed due to the advance of the inner part, i.e. crystalline part, of rhyolite lava below the Curie temperatures of magnetic minerals. This study aims to investigate the characteristics of deformation, in particular the upper part, of rhyolite lava flow during the emplacement of the lava by means of paleomagnetism. The 50-70 ka, 150 m thick Sanukayama rhyolite lava in Kozushima Island, Japan is chosen as the site of our investigation. The lava shows its vertical section due to erosion, which enabled vertical paleomagnetic sampling up to about 80 m thickness. Paleomagnetic samples were taken from pumice, welded and non-welded breccia, and obsidian in the upper grassy part. In addition, crystalline rhyolite and tuffisite (lenticular body, Isshiki, 1982) in obsidian were sampled.

Remanent magnetization of the rhyolite samples is carried by magnetite, and therefore deformation during emplacement below 580 degrees C may be detected and shows that no rotational deformation occurred after complete consolidation of the lava.

Analysis of remanent magnetization of the lava shows deflection in remanence directions by 30 degrees two times above about 400 degrees C, which is as low as the grass transition temperatures of rhyolite. Therefore, the deflection in remanence directions is interpreted as deformation of the lava after the consolidation of the upper grassy part. Assuming the deformations as being rotation about a pole, the deformations of all the grassy part can be ascribed to rotation about a single axis between temperatures of 580 and 400 degrees C. In contrast to the case for the grassy art, the inner crystalline part and tuffisite have a single thermoremanent magnetization component, suggesting that these parts are considered to have retained high temperature enough to be unaffected, i.e. above the blocking temperatures of magnetite, at the time of deformation of the grassy part.

It is concluded that using paleomagnetic data, the grassy part of the Sanukayama rhyolite lava in Kozushima Island, which was cooled below the Curie temperature of magnetite, has been rotated by the advance of the inner part of the lava during its emplacement process. In contrast, tuffisite in the grassy part of the lava is considered to have retained high temperature locally at the time of rotation of the grassy part.

Keywords: rhyolite lava, deformation, paleomagnetism, Kozushima Island

Flow directions of Miocene pyroclastic flow deposits on the northern Kii Peninsula, Japan, inferred from AMS (anisotropy of magnetic susceptibility) measurements

*Hiroyuki Hoshi[1], Masanori Ito[1]

1. Aichi University of Education

The northern part of the Kii Peninsula in central Japan was hit by a massive, widespread pyroclastic flow sometime between 15 and 14 Ma. This is based on the presence of the middle Miocene Muro pyroclastic flow deposit and its correlated deposits. To investigate the flow direction, we measured the anisotropy of magnetic susceptibility (AMS) of rock samples (n = 350) collected from 37 sites in these deposits. The samples are composed of rhyolitic-dacitic tuff (mostly welded). In general, the degree of anisotropy is not so high and the magnetic fabric is dominated by oblate (disk-like) shapes. Magnetic foliation and lineation data for the Muro pyroclastic flow deposit suggest that the flow direction as a whole was south to north but was not uniform on a local scale. Our AMS results imply a source pyroclastic vent (or vents) located to the south of Muro.

Keywords: AMS (anisotropy of magnetic susceptibility), pyroclastic flow deposits, flow direction, Miocene, Kii Peninsula

Possible existence of lava tube cave under Marius Hills Hole of the Moon

*Tsutomu Honda[1]

1. Vulcano-speleological Society

[Introduction]

The vertical pit, Marius Hills Hole (MHH), found by Haruyama has several lava layers in it's cross-section(Robinson). From a mean thickness of lava flow layers in the cross section, the yield strength of the lava is estimated by using the critical condition of free Bingham fluid flow on the inclined surface. The lava tube cave height is then estimated by the critical condition of flow between the two plates or in the circular tube and compared with the actually observed height by Haruyama and Robinson. The possible cave width by using a simple beam model from the ceiling thickness is also estimated

[Hydrodynamic model for Bingham fluid]

The lava flow model on the inclined surface with angle α is used as shown in Fig.1, where ρ is density, g is gravity, H is lava thickness and f_B yield strength of lava as Bingham fluid.

The flow critical condition of the lava is expressed as $H=nf_B/(\rho\ g \sin\alpha)$. The case for n=1,lava flows on the slope surface with a free surface, the case for n=2, lava flows between infinite width parallel plates and the case for n=4, lava flows in the circular tube (Hulme). Then,n will be between 2 and 4 for a flow in a rectangular cross sectional tube. We assumed that lava tube cave in the moon is formed as a drained flow in the circular tube or in between the parallel plates and compared with actual observation.

[Estimation of the lava yield strength and the lava tube cave height]

The depth of the MHH is 48m (Haruyama) and the cave height under MHH is 17m (Robinson), therefore the thickness of the ceiling is 31m as shown in Fig.2. The 31m thick ceiling of MHH is composed by 4 m-12 m of stratified lava layer with an average of 6 m thickness (Robinson). This average thickness H=6m is used here for the lava flow critical condition in the case of n=1 in the Rille- A. The slope angle of 0.31 deg (Greeley) , gravity g=162 cm/s^2 and density ρ=2.5g/cm^3, give an estimated value of 1314 dyne/cm^2. Consequently for n=4,H is 24m, for n=2,H is12m. As the actual cave height is 17m, so n will be between 2 and 4 with a flow in the rectangular cross-sectional tube.

[Estimation of the lava tube cave width]

It's possible to presume the cave width sustained without the ceiling's falling down for the ceiling thickness 31m by using a simple beam model with ℓ : cave width, S: tensile strength of lava, S=6.9x10^7 dyne/cm^2 (Oberbeck) and the d: ceiling thickness, For a concentrated load model (Oberbeck) , $\ell = ((4/3)\,Sd/\rho, g)^{1/2}$ =313m. For a distributed load model (Honda), $\ell = (2Sd/\rho g)^{1/2}$= 327m. If the ceiling has an arch shape, the load becomes even compressive, so the cave probably becomes wider. The flow critical condition of the lava flow in the rectangular cross section tube of hollow height 17m and width 327m will be between n=2 and n=4.

[Conclusions]

The estimated value of the lava tube cave height from this consideration is in accordance with the actual measurement. It seems that a lava tube cave of rectangular cross section with height of 17m and width of 327m exists under MHH with high possibility. The hollow detection in the MHH neighborhood by gravity measurement by Sood also suggests the existence of lava tube cave. More in-depth study and future exploration are highly expected.

References:

1)Haruyama,J. et al(2009): Geophysical Research Letters, Vol.36,L21206,2009.
2)Haruyama,J. et al(2010): 41st Lunar Planetary Science Conference,Abstract 1285,2010.

3)Haruyama,J.et al(2012): Moon,Chap6,pp139-163,Springer,2012.
4)Robinson,M.S. et al(2012): Planetary and Space Science 69,pp18-27,2012
5)Hulme,G(1974).: Geophys.J.R.Astr.Soc.,Vol.39,pp361-383,1974.
6)Greeley,G(1971):The Moon 3(1971)pp289-314
7)Oberbeck,V.R. et al(1969):Modern Geology 1969, Vol. 1, pp. 75-80
8)Honda,T(2002): Japanese speleological society Akiyoshidai meeting p34 of proceedings in 2002
9)Sood,R.et al(2015): 2nd International Planetary Caves Conference (2015)
10)Sood,R. et al(2016): 47th Lunar and Planetary Science Conference (2016)

Keywords: Vertical pit of the Moon, Lava tube, Lava cave

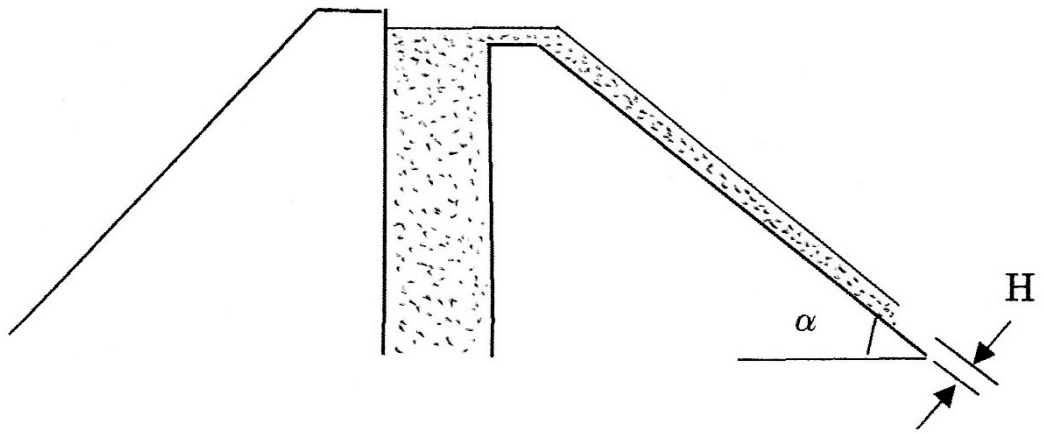

Fig.1 Critical thickness of the lava flow:$H=nf_B/(\rho g \sin\alpha)$
n=1:Free surface flow, n=2:Flow between parallel plates,
n=4:Flow in circular tube

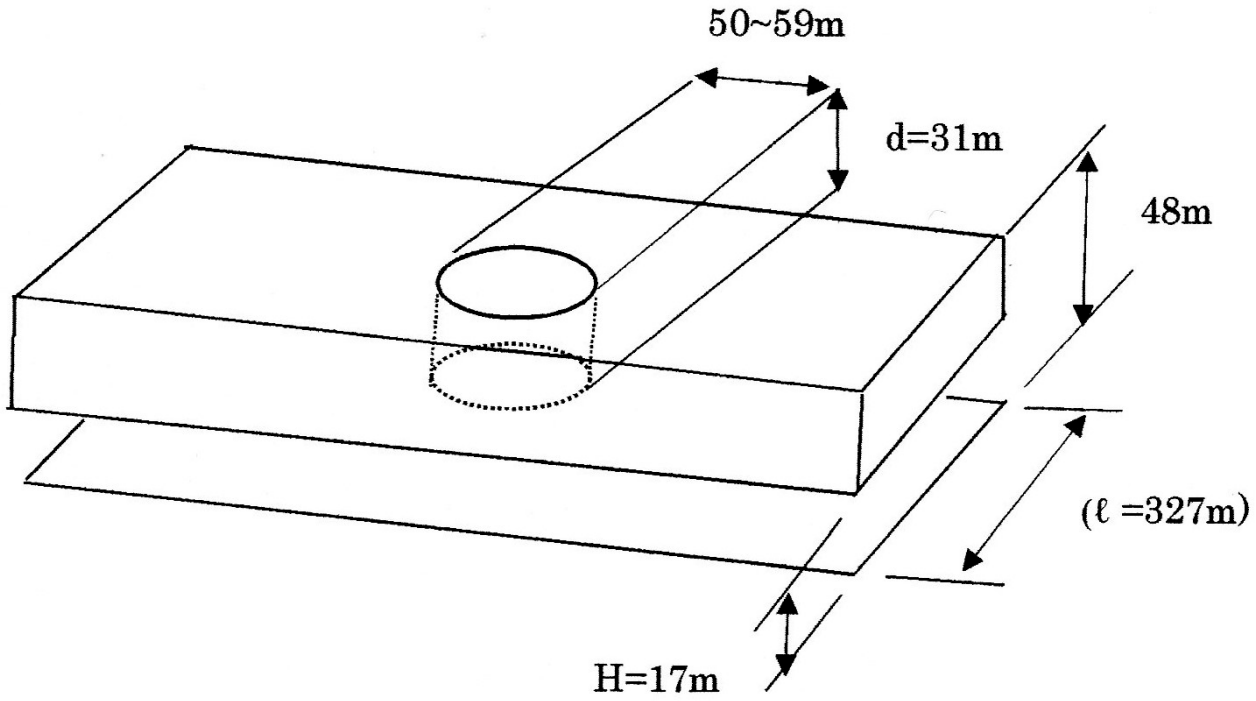

Fig.2 Schematic configuration of Marius Hills Hole

Lithofacies and Structural Development of the Sanukayama Rhyolite lava in Kozushima Island, Japan

*Kuniyuki Furukawa[1], Koji Uno[2], Kotaro Nakai[2], Tatsuo Kanamaru[3]

1. Aichi University, 2. Okayama University, 3. Nihon University

The Sanukayama rhyolite lava (Taniguchi, 1977; Isshiki, 1982; Goto et al., 2014) is distributed along the east coast of Kozushima Island, Japan. The ages are 70+/-5ka (Kaneoka and Suzuki, 1970), 110+/-30ka (Sugihara and Danhara, 2008), 46+/-3 and 68+/-5ka (Yokoyama et al., 2004). The lava is well exposed over 150m in height. The vertical lithofacies are mainly divided into the following three facies and transition zones between them. We describe the lithofacies and discuss the development processes.

*Pumiceous layer (Upper 40m)

Description: This layer is mainly composed of light gray- to pinkish-colored massive pumice with no obsidian. The pumice is partially brecciated into the elongated shape, and the clasts tend to be aligned to nearly vertically. The anisotropy of magnetic susceptibility (AMS) results show that the pumice was compacted horizontally rather than vertically.

Interpretation: The pumiceous layer was generated from effervescence of the upper part of the lava. The vertical oriented clasts and AMS results are consistent with the diapiric inflation (Fink and Manley, 1987).

*Obsidian layer (Middle 20m)

Description: The layer is composed of massive obsidian with nearly lack of microlites. The ductile-deformed light-colored veins, mainly with a few mm thick (exceptionally 1m thick) and a few to several meters long, are frequently observed. In the microscopic observation, the veins are composed of broken crystals and obsidian clasts.

Interpretation: In this layer, extensive vesiculation and microlite development would be prevented by higher load pressure and faster cooling, respectively, and resulted in the obsidian. The lava fracturing was ubiquitously occurred by flow-induced shear during ductile-brittle transition (Tuffen et al., 2003). The fractures were subsequently healed and deformed. Degassing would be promoted via the pervasive fractures, and the water contents of the obsidian layer would become heterogeneous.

*Crystalline rhyolite layer (Lower 50m)

Description: The layer is composed of light gray-colored crystalline rhyolite. The rhyolite is characterized by high vesicularity and flow banding. The vesicles are spherical shape with <1cm in diameter. The flow banding is defined by the ductile-deformed dark-colored veins, with 0.5mm thick and more than several cm long, and by aligned vesicles along the veins. The microscopic observation shows that the veins are composed of the microlite alignment associated with the surrounding spherulite trail.

Interpretation: The microlites would be developed on the healed fractures due to high heat retention comparing to the upper obsidian under large undercooling condition. Subsequently, the microlites acted as nucleation site of spherulite. The water rejection from the aligned spherulite consequently formed aligned vesicles.

*Pumiceous ~ Obsidian layers (<10m in thickness)

Description: The abundant discontinuous pumiceous layers with a few cm to 1m thick are intercalated in the obsidian. The layers tend to become thick into the upper part. The individual layers are linked each other by the pumiceous network.

Interpretation: The inhomogeneous water contents of the obsidian layer would be resulted in inhomogeneous effervescence. The pumiceous part are flattened by flow-induced shear and accumulated in upper part of the obsidian layer by buoyant force.

*Obsidian ~ Crystalline rhyolite layers (<10m in thickness)

Description: The crystalline rhyolite fragments are scattered within the obsidian layer. In the marginal part of the fragments, the vesicles show spherical shape, and spherulites are not broken at all. This indicates that the spherulites and vesicles were not deformed, and were developed after fragmentation.
Interpretation: The microlite development would induce increasing of viscosity. The high viscous microlite-rich layer would be fragmented by flow-induced shear. The spherulitic growth is subsequently occurred in the fragments as well as lower crystalline layer.

Keywords: rhyolite, obsidian, degassing, spherulite, Kozushima

Eruption event of Asama-Maekake volcano and the trial proposal of probabilistic event tree of its eruptive sequence

*Masaki Takahashi[1], Maya Yasui[1], Mitsuhiro Nakagawa[2], Minoru Takeo[3]

1. Department of Earth and Environmental Sciences, College of Humanities and Sciences, Nihon University, 2. Graduate School of Science, Hokkaido University, 3. Earthquake Research Institute, University of Tokyo

The eruption event of Asama-Maekake volcano consists of four types: (1) small scale single eruption (phreatic and phreato-magmatic), (2) intermediate scale single eruption (Vulcanian and Strombolian), (3) continuously eruptive stage (phreatic, phreato-magmatic, Vulcanian and Strombolian), and (4) large scale eruption (sub-Plinian or Plinian). A single eruption event occurs after a dormant interval of more than two years. In a continuously eruptive stage, eruptions continue for more than four years including an intercalating dormant stage of less than one year. A trial probabilistic event tree of eruptive sequence is proposed based on eruption events since 1527AD. The event tree begins with a magma intrusion detected by crustal deformation and volcanic earthquakes. The magma intrusion branches off to “no eruption” (67% probability) and “eruption” (33%). The “no eruption” event ends there. The “eruption” branches off to the “small scale eruption” (22%) and the “intermediate scale eruption” (78%). The “small scale eruption” ends there. The “intermediate scale eruption” branches off to the “continuously eruptive stage” (30%) and the “single eruption” (70%). The “continuously eruptive stage” ends there. The “single eruption” branches off to the intermediate scale eruption which ends there (88%) and the intermediate scale eruption which shifts to the “large scale eruption” (12%). The probability of occurrence of “large scale eruption” after a magma intrusion event is about 2%.

Keywords: Asama volcano, eruption, event tree of eruption

Relationship between the sequence of Eruptive episode C (Chuseri tephra) and the forming process of the Nakanoumi caldera, Towada volcano, NE Japan

*Noritoshi Izawa[1], Tsuyoshi Miyamoto[2]

1. Department of Earth Science, Graduate School of Science, Tohoku University, 2. Center for Northeast Asian Studies, Tohoku University

The Towada volcano is a double caldera volcano. The outer caldera, Towada caldera (11km diameter), was formed 15 ka. The inner caldera, Nakanoumi caldera (3km diameter), is a summit crater of the Goshikiiwa volcano, which is a basaltic post-caldera volcano. There are still several arguments for the timing of the Nakanoumi caldera formation.
The products of Eruptive episode C (6.2 ka) consist of the following three units in ascending order: Chuseri pumice (CP), Kanegasawa pumice (KP), and Utarube ash (UA); this is one of the largest activity at post caldera stage. CP is a plinian pumice deposit, KP is stratified lithic-rich pumice fall deposits, and UA is phreatomagmatic ash deposits. Although Hayakawa (1985) considered that the Nakanoumi caldera was formed in this episode from both lithic-rich features in KP and an eruptive sequence from magmatic (CP) to phreatomagmatic (UA). Because the activity at the last stage changed to phreatomagmatic eruption for almost eruptive episodes in post-caldera stage, it is difficult to discuss the timing of caldera formation from only their evidences. So to reveal the formation processes and timing of the Nakanoumi caldera, we investigated the episode C products in detail and reconstruct the eruptive sequences.
The intermittent activities of Eruptive episode C forming plinian columns suggest that these activities are independent activities with dormancy. CP is an almost homogeneous coarse pumice deposit except for the finer part at the bottom and uppermost, and this indicates that the eruption rate of the main part was constant for at least several tens hours. Lithic amount in CP deposit is constantly low in main part, but only at the top part, the lithic fragments sharply increase. The lithic fragments in KP deposits show high contents and articulate contrast. The kinds of lithic fragments in both CP and KP are rocks derived from only shallow part forming the Goshikiiwa volcano, not from deeper part. The density and chemical compositions of pumice clasts in CP and KP are constant and there are no cauliflower-like pumice clasts which show the participation of external water. The juvenile components of UA is poorly vesiculated dasitic clasts mainly and a few vesiculated particles. These features indicate that there is strong influence of external water only for UA, not so hard for CP and KP.
Macedonia *et al.* (1994) argued that the lithic fragments in tephra deposits derived from deconstruction of wall rocks by the fluid shear stress and conduit wall collapse. Roche *et al.* (2000) also argued that for small calderas like the Nakanoumi caldera, which the caldera roof aspect ratio (thickness/width) is high, high level reverse faults slice the subsiding blocks. This type caldera is considered as piecemeal type caldera by Lipman (1997). The tectonic movements by these blocks produce lithic fragments effectively and these fragments are taken by solid-gas flow in conduit. At the top of CP main part, the amount of lithic fragments increases sharply without grainsize changes, it suggests that some external factors affect the increment of lithics rather than the changes of eruptive intensity. So, it is valid that the factor is the beginning of caldera subsidence. This interpretation may explain some observed facts: the lithic-rich facies on the top of CP and KP derived from the entrainment of highly fragmented rocks around the vents by faulting; intermittent activities on KP result from the several blockades between small brocks; and the apparent changes of eruptive style between KP and UA show the inflow of external water. So, we conclude that the timing of caldera subsiding was the last stage of CP and it progressed during KP and UA.

CP emitted one eruptive column with once diminished accumulating and next grew the steady one at least half a day. In the last phase of eruption, the vent collapse occurred and started the caldera formation. Next, the eruption shifted to intermittent plinian activities (KP) with progression of subsiding. External water flew in the deepened vent and contacted with solidified magma, violent phreatomagmatic eruption occurred as UA. After these activities, the deep depression was stayed behind.
Particularly in smaller calderas like the Nakanoumi caldera, collapses take place after more than half of the total volume of the eruptive materials is already erupted (Geshi *et al.*, 2014). We constrain the timing of the beginning of subsidence and eruptive volumes. The ratio of the volume before collapse (1.86km^3) and total volume (3.04km^3), 0.63, is concordant with other smaller calderas. It suggests that the forming processes of smaller calderas are unable to explain with larger one, like Druitt and Sparks (1984).

Keywords: Towada volcano, Nakanoumi caldera, Eruptive episode C, Piecemeal type caldera

Eruptive history of Asahidake Volcano, central Hokkaido: New study of the stratigraphy and eruption ages of the products.

*Kosuke Ishige[1], Mitsuhiro Nakagawa[1], Yoshihiro Ishizuka[2]

1. Earth and Planetary System Science Department of Natural History Sciences, Graduate School of Science, Hokkaido University, 2. National Institute of Advanced Industrial Science and Technology, Research Institute of Earthquake and Volcano Geology, Volcanic Activity Research Group

Taisetsu volcano group is part of Quaternary volcanoes in the central part of Hokkaido, Japan. Asahidake is part of Taisetsu volcano group formed after the caldera forming eruption of Ohachidaira-caldera at 34 ka (Katsui *et al*,1979) and is considered as an active volcano with continues fumarolic activity. The activity and disaster response of Asahidake need to be evaluated through scientific research and observation because of many climbers and tourists visit the proximal area of Asahidake. The eruption history of Asahidake comprised of two eruptive stages of early and late stage (Ishige and Nakagawa, 2017). The early stage (until ca. 5 ka) is characterized by repeated magmatic eruptions formed a stratovolcano, while the late stage (since 2–3 ka) is characterized by phreatic eruptions. Eruptive history of the late stage activities was provided by Katsui et al. (1979) and Wada et al. (2001) and additional two radiometric ages by Okuno (2003). In addition, Holocene activities have been compiled in “The Active Volcano Summary” (ed. Meteorological Agency, 2013), but the supporting data has not been released.
To clarify the Holocene eruption history and style of the late stage of Asahidake activity, we conducted volcanic geological survey. In addition, we reported new ^{14}C dating of 4 samples to generate a more accurate cumulative volume step-diagram for eruptive magmas of Asahidake and clarified the characteristics of the history of phreatic eruptions activity over the past 5,000 years. Here, we also reported our evaluation to the long-term eruption history of Asahidake volcano.
New ^{14}C dating data revealed that the magmatic eruption ages of Asahidake west lower lavas (WL) and Asahidake Summit pyroclastic rock (SU) are cal yBP 15367-15064 and 4871–4821, respectively. The eruption rate was changed from >0.2 km^3 DRE/ky before 15 ka, to 1.0 km^3 DRE/ky, during 15 ka to 9 ka, and 0.03 km^3 DRE/ky since 9 ka to 5 ka. After 4,800 years ago, the eruption rate is considered 0 as the main eruption style became phreatic eruptions. Through detailed geological survey, we have identified two phreatic fallout depostis above SU on the proximal area. The two fallout deposits are named as Jigokudani volcaniclastic rock 1 and 2 (JD-1 and 2), in ascending order, with eruption ages are cal yBP 2845-2751 and 728-672, respectively. Eruption sequences of JD-1 were initiated by collapsed edifice producing debris avalanche which is followed by phreatic explosion. These activities formed the Jigokudani horseshoe-shaped crater. After that, lahar was effused from many small craters and fissures located in the vicinity of the opening part of the Jigokudani crater. The eruptive activity started to decrease. JD-2 eruption remarked the latest small scale phreatic eruption at North-West craters. Eruptive activity has not been frequent after the JD-1 eruption despite of the remarkable fumarolic activities. Considering the temporal change of eruptive activity, it might reasonable to infer that the activity of the Asahidake volcano has gradually decreased. However, to mitigate volcanic hazards, it should be noted that small scale of phreatic explosion and/or effusion of lahar, similar to that of JD-2 eruption, might occur near the tourism infrastructures.

Keywords: Asahidake, phreatic eruption, eruption style, eruption rate, radiocarbon dating

Omine volcano erupted just before Aso-4 pyroclastic flow

*Kousuke Shiihara[1], Toshiaki Hasenaka[1], ATSUSHI YASUDA[2], Natsumi Hokanishi[2], Yasushi Mori[3]

1. Graduate School of Science and Technology, Kumamoto University, 2. Earthquake Research Institute, University of Tokyo, 3. Kitakyushu Museum of Natural History and Human History

Eruption of Omine pyroclastic cone and effusion of associated Takayubaru lava occurred just before the caldera-forming Aso-4 pyroclastic eruption. Composition of Takayubaru lava and that of Aso-4 pumice are similar, but the former was flowing eruption, while the latter was explosive volcanic eruption. We examined the composition of phenocrysts and melt inclusions in Omine scoria, and compared composition with those of Aso-4 pyroclastic flow deposits.
Phenocrysts of Omine scoria is composed of plagioclase, clinopyroxene, orthopyroxene and opaque minerals, and scoria contain microphenocrysts of hornblende. Most of Plagioclase has honeycomb structure.
Whole-rock chemical composition of Takayubaru lava and that of Omine scoria are similar. Whole-rock chemical composition of Omine scoria overlap with that Aso-4 pyroclastic flow deposits in some elements, however they show distinct compositional trends in other elements such as TiO_2, Na_2O and MgO.
The plagioclase phenocryst composition of Omine scoria shows bimodal distribution. Main peak is An_{55} and sub peak is An_{45}. Plagioclase which has sub peak has honeycomb structure and show reverse zoning.
The clinopyroxene phenocryst composition shows unimodal distribution and normal zoning, but the orthopyroxene phenocryst composition shows normal and reverse zoning.
Composition of Omine melt inclusion in plagioclase, clinopyroxene and orthopyroxene are plotted in a narrow range of 68 - 70 wt.% SiO_2, but several melt inclusion in orthopyroxene are plotted 71 –74 wt.%.
Omine melt inclusions show distinct trends in major element vs. SiO_2 plots, and have less H_2O than Aso-4 melt inclusion.
Sr isotopic ratios of Aso-4 and Takayubaru lava are nearly equal. The results indicate that the magma supply system of Omine volcano was different from that of Aso-4. In addition, Omine magma chamber was injected magma of different composition.

Keywords: Omine volcano, melt inclusion, honeycomb structure

Petrological study of the 7.3 ka Kikai caldera-forming eruption (K-Ah), southern Kyushu, Japan

*Akiko Matsumoto[1], Mitsuhiro Nakagawa[1], Kyohei Kobayashi[1], Fukashi Maeno[2]

1. Graduate School of Science, Hokkaido University, 2. Earthquake Research Institute, University of Tokyo

Kikai caldera, located in southern Kyushu, is one of the youngest caldera volcanoes in Japan. The catastrophic caldera-forming eruption occurred ca. 7.3 ka (K-Ah eruption). It was started by a plinian eruption, followed by intraplinian pyroclastic flows (Stage 1). After that, a large ignimbrite eruption occurred, accompanied with caldera collapse (Stage 2) (Maeno & Taniguchi, 2007). This eruption was preceded by a volumetric rhyolite lava flow (Nagahama lava: NL). Although eruptive sequence of K-Ah eruption has been understood, there are few petrological studies about K-Ah eruption and therefore its magma plumbing system is still unclear. In order to understand the magma plumbing system of a large caldera-forming eruption, we carried out the petrological and geochemical investigation of K-Ah eruption including preceding activity.

The juvenile materials of K-Ah eruption are composed mainly of white pumice, and heterogeneous scoriae are also found in the upper part of Stage 2. Phenocrystic minerals are common to both juveniles of K-Ah eruption and NL, consisting of plagioclase, orthopyroxene, clinopyroxene, and magnetite. K-Ah pumice and NL have also a small amount of ilmenite. On mineral chemistry, core compositions of plagioclase in pumices show slightly wide (An40-64) with a peak of An55. In contrast, scoriae exhibit a clear bimodal distribution, mainly composed of An64-90 with a peak of An74, and a small amount of low-An plagioclase (An48-62). Pyroxenes in pumice have relatively Mg-poor cores (Mg#64-69 of opx and Mg#68-73 of cpx) and those in scoria show higher Mg# (Mg#68-73 of opx and Mg#69-78 of cpx). The plagioclase and pyroxenes in pumices show normal and reverse zoning, whereas those in scoriae exhibit weak zoning. Comparing to K-Ah pumices, NL have slightly lower-An plagioclase (An39-60), lower-Mg# pyroxenes (Mg#64-65 of opx and Mg#66-73 of cpx). On whole-rock chemistry, K-Ah pumices are rhyolitic and dacitic (SiO_2 = 70.4-73.6 wt.%), and they draw one linear trend in many Harker diagrams. Scoriae (SiO_2 = 58.1-69.0 wt.%) exhibit linear trends, which different from those of pumices. In SiO_2 vs. TiO_2 and Al_2O_3 plots, scoriae draw one linear trends, converging to dacitic end of the linear trends formed by pumices. NL are also rhyolitic (SiO_2 = 71.7-72.4 wt.%), but they are clearly different from K-Ah pumices in FeO*/MgO and Y. On Sr-Nd-Pb isotopic compositions, pumice and scoria are similar, but the former show slightly wider ranges than the latter. NL are similar to K-Ah pumices.

The heterogeneous texture of scoria and the co-existence of compositionally disequilibrium phenocrysts suggest that magma mixing is the main magmatic process in K-Ah eruption. The two distinct linear trends converging to dacitic pumice on whole-rock chemistry indicated the existence of three end-member magmas: rhyolitic, dacitic, and andesitic ones. The mixing relationship between andesitic and dacitic magmas, not rhyolitic one, as well as the co-existence of phenocrysts showing normal and reverse zoning in K-Ah pumices, suggest that there exists the silicic zoned magma chamber, in which dacitic magma stagnated beneath rhyolitic one. Andesitic magma was injected into this silicic zoned magma chamber and mixed with dacitic magma probably just before the eruption.

According to Rayleigh fractionation model, these two silicic magmas cannot be produced by simple fractionation of andesitic one. The two silicic magmas would have been generated by partial melting of crustal materials. The wide variations of isotopic chemistry of K-Ah pumices might reflect the

heterogeneity of crustal materials. The preceding activity (NL) also provided rhyolitic magma. The similarity of isotopic compositions and the difference in whole-rock chemistry suggest that NL rhyolitic magma stagnated separately from K-Ah silicic ones although their source materials are similar. In this way, the existence of multiple silicic magmas might be common in the large silicic magma system.

Keywords: Kikai caldera, large silicic magma system, multiple silicic magmas

Diversity and origin of voluminous silicic magma system

*Mitsuhiro Nakagawa[1], Akiko Matsumoto[1], Takeshi Hasegawa[2]

1. Division of Earth and Planetary System Science, Hokkaido University, 2. Faculty of Science, Ibaragi University

It has been widely accepted that large scaled silicic magma eruptions were caused by the mafic injections into large silicic magma storage system. In some cases, the mafic injection is considered as a trigger of eruption to produce mingled magma between the mafic and silicic magmas. On the other hand, it has been also discussed that a zoned magma chamber could be formed before the eruption by the mafic injection into the silicic magma chamber. In both cases, many previous studies have considered that the silicic magma was nearly homogeneous. However, we have recognized the possible diversity in the silicic magma from many large silicic eruptions. In case of caldera-forming eruption, such as 42 ka Shikotsu, 120 ka Kutcharo and 7.3 ka Kikai-Akahoya ones, voluminous silicic magma erupted with small amount of mafic magma. Thus, it has been concluded that mafic injection occurred just before eruption. However, there exists possible diversity of the silicic magma. The silicic magma shows compositional variations, ranging from rhyolite to dacite. In addition, many major and trace elements and isotope ratios exhibit single linear trend in SiO_2 variation diagrams. It should be noted that these linear trends do not continue to coexisted mafic magma, ranging from dacite to basaltic andesite. Thus, it can be concluded that mafic magma(s) injected into the silicic magma, which showed distinct, compositional variations. Phenocrystic minerals in the silicic magma can be compositionally distinguished from those derived from the mafic magma. These minerals, such as plagioclase and pyroxenes, show relatively wide variations. In addition, normally and reversely zoned phenocrysts coexist in a single silicic sample. These and linear trends in SiO_2 variation diagrams indicate that the silicic magma is mixing products between two silicic end-member magmas such as rhyolitic and dacitic ones. Considering isotope ratios of the silicic magma, these two end-member magmas were derived from distinct source materials. In addition, these silicic magmas could not be produced by simple differentiation processes from the mafic magmas. Thus, it can be assumed that the silicic magmas could be formed by crustal melting. Although crustal materials are usually heterogeneous, there should exist considerable difference in the region of crustal melting to produce contrasted two silicic end-member magmas. Analysis of compositional zoning profiles of phenocrystic minerals suggests that mixing between silicic magmas had occurred several hundred years before eruption. The mixing could form a zoned, large, silicic magma chamber, in which mafic magma injected just before eruption. On the other hand, eruptions of VEI=5 class, such as AD 1640 Hokkaido-Komagatake and AD 1667 Tarumai ones, also show small but possible compositional variations of the silicic magma, dacitic one. However, the variations are smaller than those in caldera-forming eruptions (VEI=7). This might correspond to the difference in volume of the region of the crustal melting to form silicic magma.

Keywords: silicic magma, magma diversity, rhyolite, caldera-forming eruption, crustal melting

Strategy for the long-term prediction of large scale volcanic eruptions

*Atsushi Toramaru[1], Shunsuke Yamashita

1. Department of Earth and Planetary Sciences, Faculty of Sciences, Kyushu University

It is important to understand what factors control when and how much large the next eruption occurs. In the case of relatively large scale eruptions exceeding VEI 4, the eruption is triggered by the overpressure due to the crystallization-induced vesiculation or the magma supply from below. In this talk, we propose the methodology for the long-term prediction of such large scale eruptions, which is controlled by the magma supply from below.
The historical eruptions of Sakurajima volcano, Bunmei, Anei, and Taisho, and Showa eruptions, provide the luckiest cases to investigate the long term behavior of large scale volcanic eruption because the volume of erupted material and eruption ages are exactly determined due to the best exposure of lavas and available documents. Thus, as the summary of geological studies, we have the precise diagram of cumulative volume versus time (so called "step diagram" frequently used in Japanese community). In addition, rich petrological data also show that at least two magmas mixed during the eruption intervals to shift the erupted compositions to mafic through 500 years, suggesting that two magma reservoirs, the upper felsic and the lower mafic reservoirs, exist as the stationary plumbing system beneath the Sakurajima volcano. Our recent CSD (Crystal Size Distribution) study for two types of plagioclase phenocrysts originated from these two endmember magma reservoirs reveals that the crystallization condition including nucleation, growth and settling of crystals in the upper felsic reservoir is nearly constant through the last 500 years, whereas in the lower mafic magma reservoir the supply rate from the mantle increases with time through the last 500 years. The advantage of CSD method allows us to quantitatively evaluate the supply rate of magmas from the mantle. Thus, applying the CSD method to historical eruptions, Sakurajima volcano, we can draw the curve of supply rate on the step diagram. As a result, it is found that the CSD derived-supply rate well explains the eruption times for the past eruptions. In addition, by extending the curve of supply rate to the future time and finding a point of intersection with the cumulative volume curve, we can predict when the next eruption takes place. To obtain a reliable result, we have to improve the estimation of supply rate from CSD data and examine the assumptions such as constant crystal growth rate in the CSD method.

Keywords: long-term prediction, large scale volcanic eruption, cumulative volume curve, CSD (Crystal Size Distribution)

Experimental constraints on pre-eruptive P-T conditions of Aso-4 silicic magma

*Masashi Ushioda[1], Isoji MIYAGI[1], Toshihiro Suzuki[2], Eiichi Takahashi[2]

1. Geological Survey of Japan, The National Institute of Advanced Industrial Science and Technology, 2. Department of Earth and Planetary Sciences, School of Science, Tokyo Institute of Techonology

Aso-4 is the largest and recent caldera forming eruption (>600 km^3) in the Aso volcano. In order to forecast future eruptions, understanding the magmatic process of past eruptions was very important. Determining the physical and chemical conditions (P, T, X_{H2O}, fO_2) in the magma chamber enables us to constrain trends of crystal differentiation and compare the data with geophysical observations. Kaneko et al.(2007) carried out petrological analyses for Aso-4 products systematically and discussed the conditions of magma chamber. However, pressure of the pre-eruptive conditions, which is an important parameter for the comparison to various observations, for Aso-4 products was not determined by petrological study. In this study, the purpose was determination of pre-eruptive conditions (P, T, X_{H2O}, fO_2) of Aso-4 silicic magma chamber. Reproduction of phenocryst assemblage and compositions of Aso-4A pumice (KJ5665: Hoshizumi, personal communication), which had the most silicic composition and was considered as the felsic end member, was carried out using high-P and high-T experiments.
KJ5665 pumice had plagioclase, orthopyroxene, magnetite, and ilmenite and trace of hornblende phenocrysts. All frequent distributions of core compositions for these phenocryts were unimodal. Core compositions of plagioclase and orthopyroxene ranged from An30 and Mg#72 to An50 and Mg75#, respectively. Temperature and fO_2 were 870~880 ˚C and FMQ+2, respectively, estimated by thermometer and oxygen barometer using equlibrium between magnetite and ilmenite (Lepage 2003; Andersen and Lindsley 1985). Three hydrous glasses (2.0 to 6.0 wt.% H_2O) were synthesized using the powder of KJ5665 for starting materials of high-P and high-T experiments. Melting experiments were performed in temperatures between 810 and 930 ˚C at 200, 400, and 700 MPa under NNO-buffered condition using IHPVs (SMC8600 and HARM200 installed at Tokyo Institute of Technology and Geological Survey of Japan, AIST, respectively). Plagioclase, orthopyroxene and/or K-feldspar crystallized with small amount of Fe-Ti oxides in the lower H_2O content of run products, while orthopyroxene did not crystallize and biotite crystallized in the higher H_2O content of run products. At 200 MPa and 900 ˚C and under low H_2O content (~2wt.%) of run products, plagioclase and orthopyroxene which compositions falled within the range of that of phenocrysts crystallized. In the experiments, hornblende which existed rarely as phenocrysts in the KJ5665 pumice did not crystallized. Origin of hornblende phenocrysts need to be carefully considered using various petrological features.

Acknowledgment
This study was supported by the Secretariat of the Nuclear Regulation Authority, Japan.

Keywords: high pressure and high temperature experiments, Aso-4, hydrous melting experiments, magma chamber

Collapse mechanism of small calderas: a case study of the Ohachidaira caldera, Hokkaido, Japan

*Yuki Yasuda[1], Keiko Suzuki-Kamata[1]

1. Graduate School of Science, Kobe University

In order to elucidate the collapse mechanism of small calderas, we have reconstructed the Ohachidaira caldera-forming eruption and revealed componentry of lithic fragments from the proximal products of the eruption to determine the conduit evolution. The proximal products consist of five units, from base to top: pumice and scoria fall (SK-A), climactic ignimbrite (SK-B), lithic breccia (SK-C), scoria fall (SK-D), and minor ignimbrite (SK-E). A thin fine-ash layer caps SK-C lithic breccia and is overlain by SK-D scoria fall, indicating a short hiatus in explosive activity after ejection of the lithic breccia. All units consist of dacitic pumices, andesitic scorias, and banded pumices as juvenile components. During the eruption, andesitic magma ascended alongside the conduit wall while dacitic magma ascended near the conduit center, since (1) plutonic lithic fragments are coated with scoria rather than pumice indicating that conduit and/or magma chamber walls composed of plutonic rocks attached to andesitic magma, and (2) the juvenile components in SK-A change laterally outward from scoria-rich to pumice-rich, suggesting that scoria clasts ascending alongside the conduit wall were thrown to lower heights and fell on closer to the vent while pumice clasts ascending near the conduit center reached greater heights and were transported farther. The plutonic lithic content is minor in SK-A (0%) and the lower part of SK-B (2%), and increases rapidly in the middle part of SK-B (50%) suggesting a collapse of the roof of the magma chamber. It then decreases gradually in the upper part of SK-B (26%) and decreases sharply in SK-C (2%), which probably means that the collapse propagated upwards. We postulate that SK-C lithic breccia marks conduit collapse that produced abundant lithic fragments, choked the conduit, and stopped the eruption. This hypothesis is further supported by the vertical variation of the volume ratio of pumice to scoria clasts in SK-C.

Keywords: small caldera, collapse mechanism, Ohachidaira, lithic componentry, plutonic rock

Characteristics of a plinian eruption producing caldera-collapse: an example of the 40-ka Shikotsu Pyroclastic Fall Deposit, Hokkaido, Japan

*Takahiro Yamamoto[1], Mitsuhiro Nakagawa[2]

1. Geological Survey of Japan, AIST, 2. Department of Natural History of Science, Faculty of Science, Hokkaido University

By the collapse caldera formation, there are many examples to begin with a plinian eruption prior to a large-scale pyroclastic flow eruption.
Then what is the plinian eruption not to cause that a collapse caldera is raised different in? For this problem solution, we carried out field study for the plinian pyroclastic fall deposit (Spfa1) of the Shikotsu caldera forming eruption approximately 40 ka it was the model example of the caldera collapse and particle size analysis of the deposits. Spfa1 holds a distribution main axis in the ESE direction from Shikotsu caldera and can be traced for 180 km to Cape Erimo. And its magma volume is 40 to 48 km3 DRE. The significant characteristic of Spfa1 is that the particle size distribution of the pumice particle is different from the lower part at the upper part. Thus, the upper part shows the distribution of double modes whereas the pumice particle is lognormality distribution of the single mode at the lower part. When the upper atmosphere of November in Sapporo that the wind velocity has a big are assumed, the heights of eruption-columns are 30 to 20 km and 15 to 10 for the coarse and fine modes in the upper part, respectively.
In addition, the mass ratio of the coarse mode grains is around 70 wt% along the distribution main axis, but it decreases to 30 wt% at 25km north perpendicular to the main axis. This means that the sources of both modes existed in the place of the geographically remote independence. In other words, Spfa1 which caused the caldera-collapse was a product of coincided plural plinian eruptions, and it is thought that this eruption was different from the eruption from the normal single source in beginning of eruption.

Keywords: Shikotsu caldera, plinian eruption

Re-examination of the sequence of the Early Pleistocene Shirakawa ignimbrites and their identifications in distal areas in Northeast Japan

*Takehiko Suzuki[1], Masanori Murata[2], Kiyohide Mizuno[3], Takeshi Ishihara[3]

1. Faculty of Urban Environmental Sciences, Tokyo Metropolitan University, 2. University Education Center, Tokyo Metropolitan University, 3. National Institute of Advanced Industrial Science and Technology

The Aizu volcanic region located in NE Japan is one of the Quaternary volcanic clusters resulting from the subduction of the oceanic Pacific Plate beneath the North American Plate. This volcanic region is characterised by Early Pleistocene large Shirakawa ignimbrites resulting from repeated caldera-forming eruptions and has been examined by several previous studies that established the eruptive sequence, the correlations of proximal ignimbrites with distal fall-out tephras and the eruptive history. However, the proximal sequence of ignimbrites proposed by previous studies is inconsistent with that of distal fall-out tephras, suggesting the necessity to re-examine the sequence. We present a revised stratigraphical framework of the ignimbrites included in the Nanaorezaka Formation exposed in the West Hills of the Aizu Basin, together with their petrographic description and correlations with distal fall-out tephras. From the glass chemistries and refractive indices of glass shards and phenocrysts, we identified six Early Pleistocene ignimbrites: in ascending order, the Kumado, Akai, Ashino, Nishigo, Kachikata and Ten-ei ignimbrites. In addition, the vitric widespread Kurokawa Tephra originated from a distant volcano. Four distal fall-out tephras associated with four ignimbrites (Kumado, Akai, Ashino and Kachikata) are distributed broadly in the Kanto and Niigata regions. Each combination of both the proximal and distal tephra was labelled Sr-Kmd, Sr-Aki-Kd18, Sr-Asn-Kd8 and Sr-Kc-U8, respectively. We re-examined their ages considering the stratigraphic positions of distal tephras identified in the Kanto region where calcareous nannofossil biostratigraphic and magneto-stratigraphic frameworks were available and many radiometric ages have been determined: Sr-Kmd (1.542–1.504 Ma), KK (1.533–1.485 Ma), Sr-Aki-Kd18 (1.522–1.460 Ma), Sr-Asn-Kd8 (1.219 Ma) and Sr-Kc-U8 (0.922–0.910 Ma). In addition, we estimated the volume of each fall-out tephra for Sr-Kmd, Sr-Aki-Kd18, Sr-Asn-Kd8 and Sr-Kc-U8 to be approximately 23 km3. It is concluded that the total volume of each eruptive event, except the Ten-ei eruption, ranges between 38 km^3 and 173 km^3. This indicates that these eruptions can be classified as VEI 6–7. The total volume of the Shirakawa ignimbrite and its associated fall-out tephra is 498 km^3 (DRE: 199 km^3). In addition, we estimated the eruption rate of the tephra associated with caldera-forming eruptions during the period from the Sr-Kmd to Sr-Kc-U8 eruptions to be 0.3 km^3/kyr in DRE, an average value for the Quaternary volcanoes in the area of the Japanese Islands. The four repose periods between the successive eruptions were variable, ranging from approximately 0.3 My to less than 0.08 My.

Keywords: Shirakawa iginimbrites, Early Pleistocene, Northeast Japan, caldera forming-eruption, widespread tephra

Distribution and eruptive volume estimation of Ito, Hachinohe and Aso4 pyroclastic flow deposits

*Shinji Takarada[1], Takashi Kudo[1], Nobuo Geshi[1], Hideo Hoshizumi[1]

1. Geological Survey of Japan, National Institute of Advanced Industrial Science and Technology

Estimation of distribution and eruptive volume of large to middle-scale pyroclastic flows are important for evaluation of affected area and emplacement processes of pyroclastic flows. Distributions and eruptive volumes just after the eruption were estimated at Ito pyroclastic flow deposit derived from Aira caldera (30ka), Hachinohe pyroclastic flow deposit derived from Towada caldera (15ka) and Aso4 pyroclastic flow deposit derived from Aso caldera (90ka). The eruptive volumes of tephra falls derived from pyroclastic flows (co-ignimbrite ash) are not included for the estimation.
The distributions of pyroclastic flow deposits just after the eruption were made by the following method. (1) made current distributions of pyroclastic flow deposits using geological maps, and published research papers, (2) made upper and lower elevations and thickness point datasets using boring (drilling) data (eg. Kunijian and Geo-Station), published papers and geological maps, (3) convert deposit thickness into non-welded from welded part (eg. 1000kg/m^3 of non-welded, 1700kg/m^3 of weakly welded, 2000kg/m^3 of highly welded at Ito pyroclastic flow deposit), and (4) estimate distribution of submarine area with the consideration of sea-level at the time of eruption (Ito: -100m, Aso4: -50m). For example, the energy cone simulations were used to estimate the maximum travel distances in the sea area for Ito pyroclastic flow. The energy cone parameters of Ito pyroclastic flows were H/L=0.005-0.014 and column collapse height=1050-1200m. The eruptive volume were estimated by the following method. (1) made 5km or 1km mesh data, (2) calculate the distribution area of pyroclastic flow deposit in each mesh, (3) calculate maximum, average and minimum point thickness datasets in each mesh, (4) If no point data were available in the mesh, the Kriging method were used to estimate the thickness value in the mesh, and (5) the total volume were estimated from the sum of multiply the area by the thickness data of each mesh (maximum, average and minimum cases).
The estimated eruptive volumes of Ito pyroclastic flow with 1km mesh were 325km^3(max), 200km^3(ave) and 130km^3(min) in DRE. The estimated volumes of outflow deposit (except the within the caldera deposit) were 250km^3(max), 125km^3(ave) and 50km^3(min) in DRE. The estimated volumes of Hachinohe pyroclastic flow (outflow deposit) with 5km mesh were 27km^3(max), 20km^3(ave) and 13km^3(min) in DRE. The estimated volumes of Aso4 pyroclastic flow with 5km mesh were 530km^3(max), 370km^3(ave) and 200km^3(min) in DRE. The estimated volumes of outflow deposit were 400km^3(max), 270km^3(ave) and 140km^3(min) in DRE. The thickness of the point data sets was reduced due to erosions; therefore, the reliable eruptive volumes of pyroclastic flows were considered between maximum and average estimations. The more precise estimation of original surface and basal topography of the pyroclastic flow deposits and evaluation of distribution in the sea area are the important key factors for the estimation of eruptive volume of large-scale pyroclastic flow deposits (The above estimated volumes are provisional; the values may change due to further studies).

Keywords: Pyroclastic flow, Distribution, Eruptive Volume, Ito, Hatchnohe, Aso4

Volcanic activity and magma plumbing system during caldera and post-caldera stage of Mashu volcano, eastern Hokkaido

*Keiji Wada[1], Yu Nakatsuka, Eiichi Sato[2], Yuya Okada[1]

1. Earth Science Laboratory, Hokkaido University of Education at Asahikawa, 2. Institute for Promotion of Higher Education, Kobe University

Mashu volcano, characterized by a caldera of 6 x 7 km diameter generated about 7500 years ago, is located at eastern ridge of Kutcharo caldera in the Akan-Shiretoko volcanic chain in eastern Hokkaido (Katsui et al., 1975). Mashu volcano started activities around 35 thousand years ago and has repeated explosive eruptions many times (Sumita, 1990; Hasegawa et al., 2009). Volcanic sequence of caldera stage and post-caldera stage during 14 thousand years has been well studied by Kishimoto et al. (2009) based on previous research of Katsui et al. (1975 and 1986). However, magma plumbing system during caldera stage and the following post-caldera stage, and stratigraphic relationship between post-caldera lavas and tephra deposits have not been cleared by petrological approach. We show plural magma chamber models at the caldera stage and eruptive sequence of post-caldera stage including four lavas. Major caldera formation of tephrostratigraphy of Ma-j, Ma-i, Ma-h, Ma-g, Ma-f (Kishimoto et al., 2009) was reviewed. According to the change of lithic fragments and existence of lithic-rich thin layers between pumice fall deposits, the location of the crater may have changed during the plinian eruptions. The most mafic compositions of bulk and minerals in Ma-g tephra has different compositional trend compared with other eruptive products of caldera-forming series. Ma-f large-volume pyroclastic flow deposit shows a wide compositional variations including the range of all other caldera-forming series products. These suggest existence of two different magma chambers of Ma-j, Ma-i, and Ma-h units and of Ma-g unit. It seems that both of the magma chamber eventually reached the catastrophic eruption of Ma-f unit. During the post-caldera stage (6000?-1000 years ago) magma activity was changed to the new plumbing system based on the bulk chemistry. Kamuishu-island lava dome (SiO_2=73.9wt.%) in the center of the caldera erupted at the beginning of a long dormant period after the caldera formation, after that Kamuinupuri small strato-cone was formed in the eastern edge of the caldera. The eruptive sequence of three lavas from Kamuinupuri was deduced by bulk and minerals chemistry. Kamuinupuri northwestern lava (SiO_2=68.5wt.%) erupted during the main activity of Kamuinupuri strato-cone formation (Ma-d tephra; SiO_2=63.9-69.4wt.%). After the Ma-d tephra activity Kamuinupuri western lava (SiO_2 =54.5-61.6wt.%) effused. The Kamuinupuri north lava (SiO_2=70.6wt.%) can be erupted after the Ma-c tephra layer eruption (2500-1500 years ago). At about 1000 years ago the latest explosive eruptions including plinian fall and pyroclastic flow (Ma-b tephra; SiO_2=67.0-69.3wt.%) occurred.

Keywords: Mashu volcano, caldera, magma plumbing system

Investigation on Funatsu Tainai lava tree molds in Kenmarubi-I lava flow

*Tsutomu Honda[1], Hiroshi Tachihara[1], Tadato Makita[1]

1. Vulcano-speleological Society

[Introduction]

Funatsu Tainai lava tree molds are a national natural monument located in the midstream area of Kenmarubi-I lava flow, and their measurement and investigation were carried out by K.Ogawa of Speleological Society and published as Yamanashi-ken natural monument urgent investigation report[1)]. The investigation is continued and new additional lava tree molds are found and named as Yamanashi-ken monument important material by NPO Vulcano-Speleological Society. The volcanologic knowledge obtained from the current state of those investigations will be reported.

[The lava flow thickness and yield strength]

Funatsu Tainai lava tree molds count many vertical lava tree molds among which main natural monument and monument important material are listed in Table.1. The depth of the vertical tree mold are between 2.1m and 5.4m. Most has 4 m-5 m of depth as shown in Table.2. A diameter of a tree in this area was at most 1.9 m. The depth of the vertical lava tree molds shows a lava flow thickness. H, and gradient angle α in this area is approximately 8 degree, so the Bingham yield strength:f_B can be estimated as f_B =6.9x104~1.9x105dyne/cm^2 from lava flow critical condition :H=f_B/ (ρ g sin α) of simple lava flow where ρ=2.5g/cm^3 and g=980cm/sec^3. This f_B is regarded as the proper value as basaltic lava of SiO_2 50.88wt% (Tsuya [4)]) or 51.1% (Takada [5)]), though it seems a little bit high because of the temperature fall at this area. This value agree with estimated value 5.0x10^4~1.5x10^{5}dyne/cm^2 by Yamashita [6)]. Therefore Kenmarubi-I lava flow can be regarded as a simple lava flow defined by Walker [7,8)].

[Lava rib structure and surface tension estimated in Tainai]

Funatsu Tainai shows a complex lava tree molds which include lava stalactite from the ceiling and the ribbed wall formed by re-melting inside it[9)]. It's possible to estimate the surface tension of the lava from the pitch of the lava stalactite and ribbed wall[10)]. From instability onset conditions of melted liquid thin film, pitch(wave length) is shown as P=2 π(γ/g ρ)$^{1/2}$,where γ is the surface tension of the lava and g is the gravity, and ρ is the density of the lava. Therefore it's possible to estimate a surface tension γ = P^2 g ρ /4 π^2 by measuring P of lava stalactite which hangs down from the ceiling inside the Tainai or from ribbed structure of side wall. The pitch obtained from Funatsu Tainai indicated in Fig.1 is P=3~4cm approximately, then, γ=560-990 dyne/cm is obtained as the surface tension. It's the reasonable value as surface tension of basaltic lava.

[Conclusion]

Similar results of yield strength and surface tension are also obtained for the Yoshida Tainai lava tree molds in the lava flow of Kenmarubi-II(SiO_2 51.2wt%[5)]). Kenmarubi-I and the Kenmarubi-II are regarded as a simple lava flow. These lava flows has so low thickness that could not make a lava tube cave. Without being buried, much of lava tree molds are left. So, the biggest complex lava tree mold in the world exists in this area[3)]. On the other hand, Aokigahara lava flow which has thick lava flow and high flow rate making a lot of lava tube caves indicates a compound lava flow. Further researches and investigations are under going for both Tainai lava tree molds.

References:

1) Yamanashi-ken natural monument urgent investigating committee and lava cave/tree mold are an investigation group of Ogawa:Yamanashi-ken natural monument urgent investigation report (1996), Yamanashi-ken Education Board , p182-344.

2) H.Tachihara,T.Makita (1998): 1997 1998 year lava tree mold report,NPO Vulcano-Speleological Society.
3) H.Tachihara (2011): Volcano cave and lava tree mold. Caving journal No.43,p15-17
4) H.Tsuya(1971): The geographical feature of Mt. Fuji and the geological feature. Mt. Fuji overall investigation report, Fuji Kyuko p71
5) A.Takada et al (2016): Fuji volcanic geologic map (2nd edition), National Institute of Advanced Industrial Science and Technology ,Geological Survey of Japan.
6) S.Yamashita et al (2002): Reproduction of the Kenmarubi Lava Flow by a Numerical Simulation :. Japan Geoscience Union Meeting V032-P022
7)G.P.L.Walker(1971):Compound and simple lava flows and flood basalts. Bull.Volcanol.35,p579-590
8) S.Umino (2007): Characteristics of Lava flows of Fuji volcano, Fuji Volcano, Yamanashi Institute of Environmental Sciences p269-283
9) T.Honda (1998): Physico-chemical Explanation for Remelting Process of Inner Surface Wall of Tainai Tree Molds Located on the Flank of Mt. Fuji. Journal of the Speleological Society of Japan,vol 23,p29-38
10) T.Honda (2015): Estimation of surface tension of lava from lava stalactite and lava stalagmite appeared in lava tube cave and tree mold. Japan Geoscience Union Meeting SVC46-07

Keywords: Lava tree mold, Kennmarubi-I lava flow, Funatsu tainai

Table.1 船津胎内縦樹型の深さと直径
（文献 1）から縦樹型のみを抽出したもの）

船津胎内縦樹型番号	深さ	直径
No, 1	3. 0m	1. 3m
No, 3	4. 9m	0. 6m
No. 4	4. 9m	0. 9m
No. 5	3. 0m	1. 3m
No. 6	4. 0m	1. 2m
No. 7	3. 6m	0. 9m
No. 8	3. 9m	1. 2m
No. 10	4. 3m	1. 5m
No. 12	4. 3m	0. 6m
No. 14	4. 9m	0. 6m
No. 18	5. 4m	1. 0m
No. 19	4. 8m	0. 8m
No. 21	4. 0m	1. 2m
No. 24	3. 0m	1. 3m
No. 25	5. 2m	0. 8m
No. 26	4. 6m	0. 6m
No. 29	3. 3m	1. 3x2. 7m
No. 38	2. 1m	0. 9m
No. 39	2. 3m	1. 6m
No. 40	2. 3m	0. 3m
No. 41	2. 9m	1. 6m
No. 42	4. 9m	1. 3m
記念物重要資料 No. 3	3. 9m	1. 1m
記念物重要資料 No. 105	2. 9m	1. 9m

Table.2 船津胎内縦樹型の深さと本数の分布

縦樹型の深さの範囲	樹型の本数
2. 0m-2. 9m	5
3. 0m-3. 9m	7
4. 0m-4. 9m	10
5. 0m-5. 4m	2

Fig.1 船津胎内の肋骨状溶岩とピッチの計測

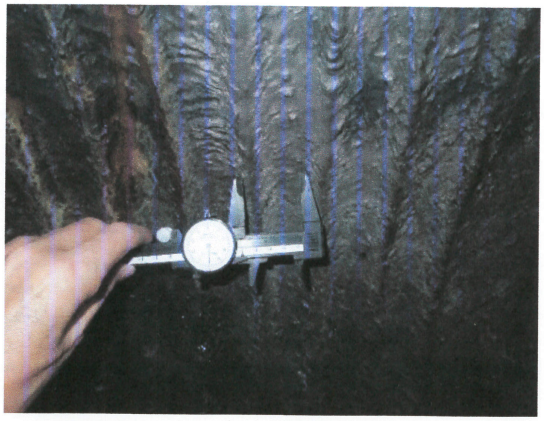

Frequency of volcanic eruptions and long-term magma discharge rate in sub-regions in Japan

*Koji Kiyosugi[1]

1. Organization of Advanced Science and Technology, Kobe University

Frequency of volcanic eruptions is an important factor to evaluate volcanic activity. Together with eruption magnitude, which is defined by mass of ejecta, frequency of eruptions can be used to estimate long-term magma discharge rate. Such estimation will provide an insight of material circulation through volcanoes. Calculating frequency of eruptions is, however, a challenging problem due to difficulty of estimating the amount of under-recording of volcanic eruptions. The main mechanisms of under-recording are absence of historical records, erosion and alteration of tephra deposits, burial of tephra deposits by younger deposits, disappearance of the source volcano itself due to burial or erosion, deposition of majority of tephra on the sea surface and occurrence of submarine eruption. In this study, I calculated frequency of volcanic eruptions and estimated long-term magma discharge rate in sub-regions in Japan, in which eruption records account for about 39 % of the entire set of eruptive events in the world.

I investigated the dataset of age and magnitude, *M*, of volcanic eruptions (*M* 2), which occurred in the Hokkaido, Tohoku, Izu, Central and Kyushu regions in Japan in recent about 2 million years. The analyzed data are compiled from documentation including Machida and Arai (2003), Committee for Catalog of Quaternary volcanoes in Japan (2000), Geological Survey of Japan, AIST (2014) and Hayakawa (2010). In estimating frequency of eruptions, under-recording of events was taken into account by modeling a decreasing trend of recording rate of analyzed volcanic eruptions with time.

The results of the analysis show that the frequency of eruptions (*M* 2) in those regions varies more than one order of magnitude. For relatively large eruptions (4 *M* 6), frequency of eruptions decays by a factor of about 10 for each successive eruption magnitude category. On the other hand, frequency of eruptions (2 *M* 4) decays by a factor of about 1.5 - 2.6, showing that the frequency of smaller eruptions is smaller than the frequency expected from the magnitude-frequency relationship of the relatively larger eruptions. One possible explanation of this small frequency is that smaller batch of magma is less buoyant and is more likely stuck in the crust.

The long-term magma discharge rate was calculated on the basis of the magnitude-frequency relationships in those regions. After considering the length of those subduction zones, the long-term magma discharge rate in Kyusyu, Central and Tohoku regions show similar value (2×10^{10} kg/ka/km). On the other hand, the long-term magma discharge rate in Hokkaido and Izu regions is about one third of that of the other regions. The smaller long-term magma discharge rate in the Hokkaido region than that in the Tohoku region is probably caused by an oblique subduction of the Pacific plate, which results in a smaller effective subduction velocity of the Pacific plate beneath the North American plate in the Hokkaido region than that in the Tohoku region. On the other hand, the similar amount of long-term magma discharge rates in different subduction zones, including the Tohoku, Central and Kyushu regions, suggest that such tectonic constraint is not significant. Furthermore, the estimated small magma discharge rate in the Izu region may be caused by insufficient estimation of the amount of under-recording of events. This region consists of small volcanic islands where wide-spread tephra deposits are less likely preserved, and hence eruptions in large eruption magnitude categories (*M* 6) are almost completely missing. In addition, no

eruptions are recorded for some submarine volcanoes in this region. For these missing eruption categories and volcanoes, it is impossible to estimate the amount of under-recording of events. Therefore, additional statistical approach is required for more accurate estimation of frequency of eruption and long-term magma discharge rate in the region of oceanic islands.

Keywords: eruption database, frequency of eruption, long-term magma discharge rate

Formation process of the Omine pyroclastic cone in Niijima Island, Japan

*Reina NAKAOKA[1], Kazuhiko Kano[2], Keiko Suzuki-Kamata[1]

1. Kobe University, 2. Kagoshima University

On the Niijima Island, rhyolitic eruption started in 886 with generation of the Habushiura pyroclastic density current deposits followed by the growth of the Omine pyroclastic cone and the emplacement of the Mukaiyama lava. Sedimentary structures, emplacement temperatures and ash morphology indicate the Habushiura pyroclastic density current deposits were generated by shallow marine phreatomagmatic eruption (Nakaoka and Suzuki-Kamata, 2015). In this study, we discuss the eruption style and development of the Omine pyroclastic cone with sedimentary features of the deposits and paleomagnetism of the essential rock fragments.

The Habushiura pyroclastic density current deposits constitute a plateau rising over 100 m above sea level and the Omine pyroclastic cone rises 200 m above the plateau with a basal diameter of 2.7 km, without any indication of significant time break between the Omine pyroclastic cone such as weathered zone and structural disconformity. The summit is relatively flat being covered with the Mukaiyama lava but at least, five craters are confirmed in the eastern half.

The eruption products contain block-sized to lapilli-sized poorly to moderately vesicular fragments and blocky to platy ash particles of biotite rhyolite with minor accidental fragments. Juvenile fragments contain elongate vesicles but have a bulk density of 1.6–1.7 g/cm^3, larger than 0.8–1.3 g/cm^3 for the Habushiura pyroclastic density current. These clasts are accumulated in the cone commonly to form massive, poor sorted beds abundant in ash with a thickness of several 10 cm to 120 cm thick.

Upon thermal demagnetization, magnetization direction of the juvenile fragments becomes stable and parallel to the direction of the Earth’ s magnetic field of that time below 350-400 degree C. This implies that the juvenile fragments were emplaced below 350-400 degree C and magnetized while being cooled to the ambient temperature, consistent with that block-sized juvenile fragments have prismatic cracks and are occasionally disintegrated along the cracks.

These results collectively suggest that the Omine tuff cones are composed of the pyroclastic density current deposits produced by explosive interaction between the hot lava and external water or gravitational collapse of lava. The Habushiura pyroclastic density current deposits are also interpreted as the products of explosive interaction between the hot lava and external water but its emplacement temperature is below 300 degree C as estimated also by thermal demagnetization (Nakaoka and Suzuki-Kamata, 2015). This perhaps reflects lesser extent contribution of the ambient water to the eruption of Omine pyroclastic cone. Pyroclasts, however, could accumulate to build a pyroclastic cone but exceptionally where wet in direct contact with water vapor (Aranda-Gomez and Luhr, 1996; Kano and Takarada, 2007).

The effect of open water for flow and depositional mechanisms of Koya pyroclastic flow: an examination from the ignimbrites distributed on Tanega-shima

*Tomomi Yamane[1], Keiko Suzuki-Kamata[2]

1. Graduate School of Science, Kobe University, 2. Kobe Ocean-Bottom Exploration Center

Koya pyroclastic flow (Ui, 1973) is a large-scale pyroclastic flow occurred at the 7.3 ka (Fukusawa, 1995) Akahoya eruption of Kikai caldera. Akahoya eruption started from large-scale Plinian eruption which formed plinian pumice-fall deposit and intraplinian pyroclastic-flow deposit and terminated with eruption of Koya pyroclastic flow (Machida and Arai, 2003; Maeno and Taniguchi, 2007; Fujihara and Suzuki-Kamata, 2013). The Koya ignimbrite is distributed over the proximal islands (Iwo-jima and Take-shima) and the adjacent islands (Tanega-shima, Yaku-shima and Kuchinoerabu-jima) and the mainland of south Kyusyu (Satsuma and Osumi peninsulas) around Kikai caldera (Ui, 1973; Machida and Arai, 1978; Ono et al., 1982; Maeno and Taniguchi, 2007; Geshi, 2009; Fujihara and Suzuki-Kamata, 2013).

Although it is clear that Koya pyroclastic flow traveled across the sea because of the distribution of the ignimbrite and study of the Holocene relative sea-level change (e.g. Tanigawa et al., 2013), there is no discussion about the effect of open water for Koya pyroclastic flow.

Products of Akahoya eruption contain two types of volcanic glass shards. The one is “high-SiO_2 glass shards” (ca. 75 SiO_2 wt. %), and the other is “low-SiO_2 glass shards” (ca. 65 SiO_2 wt. %). The ratio of both types of glass shards shows vertical variation within the Koya ignimbrite (Fujihara and Suzuki-Kamata, 2013). Based on the ratio of both types of glass shards, Fijihara and Suziki-Kamata (2013) concluded that the early phase products of Koya pyroclastic-flow eruption contain only high-SiO_2 glass shards and low-SiO_2 magma started to erupt at later phase of the pyroclastic flow eruption.

To reveal the effect of open water, we adopted these methods, geological survey, chemical analysis of glass shards and thickness and pumice size measurement.

For chemical analysis of glass shards, matrix samples of the Koya ignimbrite on Tanega-shima in 4 sites were sampled from base to top with regular level interval. 40-100 glass shards were selected at each level and measured the major element composition by EPMA. While high-SiO_2 glass shards can be recognized throughout the ignimbrite, low-SiO_2 ones exist only at the upper level of it. The early phase products of Koya pyroclastic-flow eruption reached to Tanega-shima because this vertical variation is equal to that of the ignimbrites on proximal area, Satsuma peninsula and Osumi peninsula (Fujihara and Suzuki-Kamata, 2013). Lower contents of low-SiO_2 glass shards from upper most level compared with that of Osumi peninsula suggest that the flows which contain abundant in low-SiO_2 glass shards occured at the later phase of the pyroclastic flow eruption cannot reach to Tanega-shima. This is conformable the fact that the ignimbrites on Osumi peninsula are thicker than that of Tanega-shima.

The maximum pumice size (MPS) was measured from the Koya ignimbrites of Satsuma peninsula, Osumi peninsula and Tanega-shima. Proportional connection between MPS and distance over water (see Figure) suggests that Koya pyroclastic flow was experienced the successively selective loss of large pumice during traveling over water. From this proportional connection, the distal limit of Koya pyroclastic flow traveling over water estimated approximately 70 km from source (see Figure). Tanega-shima is located in almost the distal limit.

Based on above discussion, it is easy to estimate that Koya pyroclastic flow lost a great many amount of pyroclasts in the sea during traveling across the sea and the Koya ignimbrite widely lies on the sea floor

around Kikai caldera.

Keywords: Kikai caldera, Koya pyroclastic flow, the effect of open water, volcanic glass shards, Tanega-shima, distal limit of pyroclastic flow

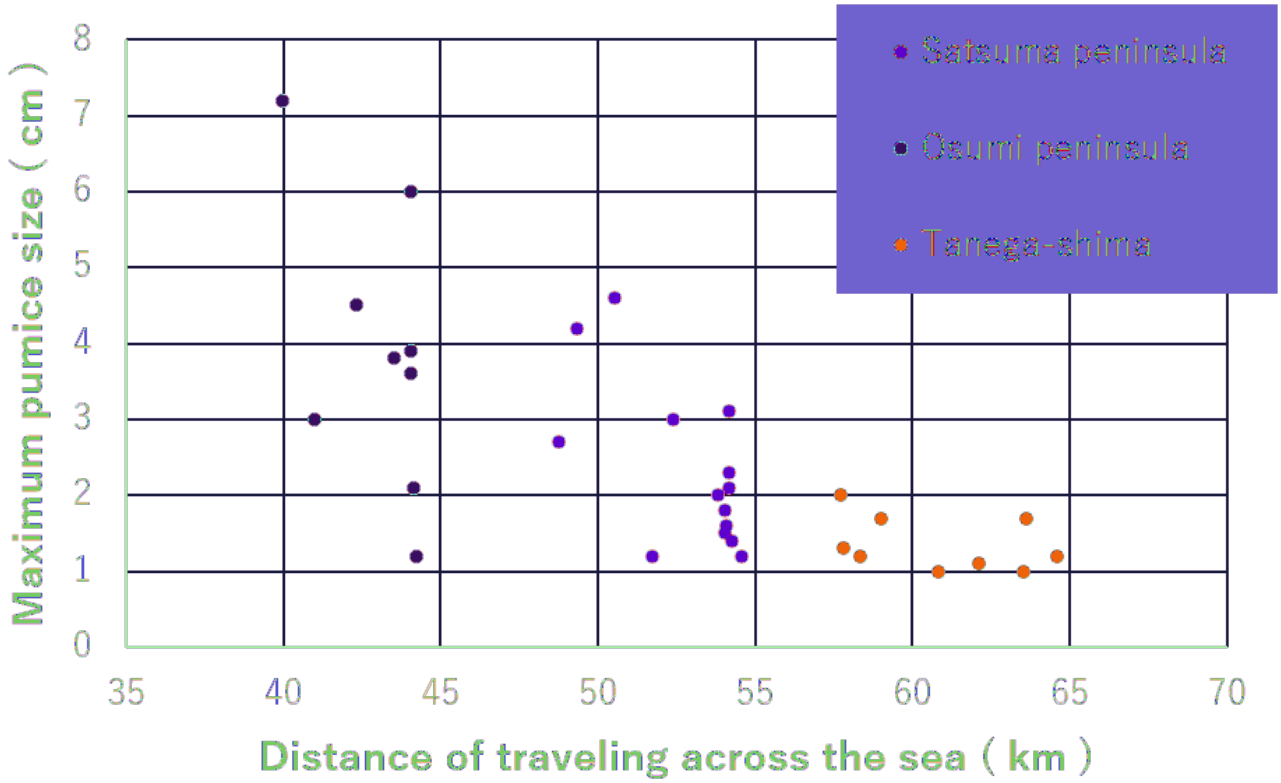

The distribution of Ikezuki tuff (Onikobe-Ikezuki tephra) in Shinjo and Mukaimachi basin, NE Japan

*Tsuyoshi Miyamoto[1], Yoshimi Hiroi[2], Masayoshi Fujino[3]

1. Center for Northeast Asian Studies, Tohoku University, 2. Graduated school of Science, Tohoku University, 3. HIGASHI NIPPON BROADCASTING CO,Ltd.

Within Shinjo basin in Yamagata prefecture, some of pyroclastic flow deposits are intercalated in gravel layer of Quaternary Systems. Especially the oldest and thickest pumice tuff (Torigoe tephra) in upper Yamaya formation is corresponded to Ikezuki tuff (Onikobe-Ikezuki tephra: O-Ik) distributing in Naruko-Onikobe area at the eastern side of the Ou Backbone range in Miyagi prefecture. From an eruption age of O-Ik, pyroclastic flow deposits and upper Yamaya formation in this basin are thought to be younger than 0.3 ka. Matu’ura (2003) devided pyroclastic flow deposits over Torigoe tephra (O-Ik) into four tephra layers (Sakekawa, Izumikawa, Emakawa and Ushikuguri in ascending order). Large-scale pyroclastic eruption is only from both Naruko and Onikobe caldera since 0.3 ka around Shinjo basin. Though three large-scale pyorclastic flow deposits (Shimoyamasato, Nisaka, Yanagisawa tuff in ascending order) are observed after O-Ik within Naruko-Onikobe area, there is a possibility that only Shimoyamasato tuff distributes in Shinjo basin because Ushikuguri tephra, which is the youngest pyroclast, is covered with Dokusawa tephra (0.1 Ka). However four pyroclastic flow deposits are not correlated with Shimoyamasato tuff in previous studies, and the source of their flow deposits are unknown. Thus to clarify the source caldera of pyroclasts in Shinjo basin, we studied the pyroclastic flow deposits within both Shinjo and Mukaimachi basin based on the field survey and petrological studies (volcanic glass and mineral compositions analysis, bulk chemistry of essential pumice fragments). In consequence we report that Torigoe tephra is not O-Ik and all pyroclasts in upper Yamaya formation are older deposits than O-Ik tephra. In this study to avoid confusion, we use “Shinjo tuff” as a newly name, not Torigoe tephra.
From the field survey pyroclastic flow stratigraphy was identified to be nearly similar to one of Matsu’ura(2003) except for one flow unit. Shinjo tuff, is the oldest and resemble to O-Ik, thickly distributes in all area of Shinjo basin. Although Emakawa tephra has as a same distribution as Shinjo tuff, the thickness decreases from north to south. No pyroclastic deposits are corresponding to Simoyamasato tuff as same as previous studies. Within Mukaimachi basin we could observe that Shimoyamasato tuff overlay the O-Ik. Though Gravel layer under O-Ik intercalates one pyoroclastic density current, five pyroclastic flow deposits within Shinjo basin are not present.
Shinjo tuff has similar features to O-Ik in field occurrence. Additionally volcanic glass compositions and heavy mineral assemblages using for tephra identification are nearly same between two pyroclasts, and Shinjo tuff was assumed to be same deposit as O-ik. But this study has determined to be two distinct pyroclasts from the difference of below three features.
1. Stratigraphy: though both O-Ik within Naruko-Onikobe area and Shinjo tuff was assumed directly to cover with the same volcanic ash layer, it was found that their ash layers are another deposits because they have distinct glass chemical composition. In addition O-Ik within Mukaimachi basin is covered by Simoyamasato tuff, while Shinjo tuff within Shinjo basin is overlain by other tuff.
2. Modal composition of heavy minerals: the contents of heavy mineral in Shinjo tuff are significantly lower than one of O-Ik.
3. Bulk chemical compositions of essential pumice fragments: despite of the effect of alternation two pyroclasts are distinguished in major element compositions, and are clearly divided in trace element composition, especially HFSE and Y which is not affected by the alternation.
O-Ik exists within Mukaimachi basin, not within Shinjo basin in the western side from source caldera. This

distribution implies that the flow path of O-Ik was limited by the western wall of Mukaimachi caldera. No distribution within Mukaimachi basin of five pyoroclastic flow deposits observed in Shinjo basin indicates that all pyrocalasts in upper Yamaya formation was older than O-Ik, this is very important to construct the evolution of Shinjo basin. Moreover it is possible from this insight that tuff in Yamaya formation were erupted from other caldera, not Naruko and Onikobe caldera. Especially the thickness changes of Emakawa tephra and Shinjo tuff might suggest that former tuff was derived from Sanzugawa caldera located on northern part of Shinjo basin, and later tuff was from Mukaimachi caldera.

Keywords: Ikezuki tuff, Shinjo tuff, Mukaimachi caldera

The source of Kamafusayama pyroclastic deposits and debris avalanche deposit, southern Fukushima prefecture, Japan

*Daisuke Sekine[1], Takeshi Hasegawa[1]

1. Ibaraki University Major in Science Department of Earth Science

1. Introduction
Kamafusayama pyroclastic deposits (KfPD, 0.59-0.41Ma)[2)3)4)] consist of dacitic to andesitic pyroclastic fall and flow deposits, distributed in the southern Fukushima. The main part of KfPD compose Kamafusayama (1510m.a.s.l). The KfPD has intermediate characteristics with respect to: 1) age, 2) distribution and 3) compositions between early Pleistocene felsic large-scale pyroclastic flow deposits (Shirakawa pyroclastic flow group, about1.51Ma-0.92Ma)[1)2)5)6)] and basaltic to andesitic Nasu stratovolcanic group (0.54Ma[7)] -present). Although clarifying the eruption history and magma processes of KfPD is essential for understanding the volcanism and magmatism in this area, detailed stratigraphy and source area have not been clearly revealed. We have carried out geological and petrological study of KfPD to reveal the stratigraphy and magmatic processes, and current results can be summarized as follows; 1) KfPD is divided into two eruption stages (Eruption stage 1 and 2) separated by a paleosol layer, 2) A debris avalanche (KfDa) deposit was found at the top of Eruption stage 1, 3) Compositional trends of Stage 1 and 2 are slightly different each other on K2O-SiO2 diagram, and 4) magma mixing was a common process in each stage.
In order to determine the source of KfPD, we investigated distributions and lateral change of thicknesses of the deposits. In addition, we compared the petrologic features (petrography and whole-rock chemistry) with adjacent volcanic rocks; Ksv (Kashi volcanic rocks (after 1.47~1.21Ma)[1)6)]) which is the older products of Kashiasahidake Volcano, Kav (Kashiasahidake Volcano(0.54Ma)[7)]) forming present edifice of Kashiasahidake Volcano, and Oshiromoriyama Lavas intruding in Ksv(Early Pleistocene)[1)]. In addition, petrologic characteristics of lava fragments in KfDa were also determined.
2. Field occurrences
Both of Eruption stage 1 and 2 of KfPD consist of alternative units of pyroclastic flow and fall deposits (Eruption stage 1 and 2 are composed of 7 and 13 units, respectively). There is no paleosol layer within the units in one stage. The thickness of KfPD air-fall units increase towards Kashiasahidake Volcano. KfDa is composed of tuffaceous matrix facies and block facies. The former contains white pumice, gray pumice, scoria, and lithic fragments of tuff and lava. The latter is materials incorporated from underlying layers and mega blocks (max 3.0m in diameter) of andesitic lava. KfDa is deposited in northeastern and southeastern sides of Kamafusayama. Maximum thickness is 7.0 m at the northeastern side of Kamafusayama.
3. Petrographic characteristics and discussion
Common phenocryst minerals of Ksv, Kav, KfDa and Osd are Pl, Opx, Cpx, Opq. Some samples of KfPD, Ksv and Osd include Qtz phenocryst. Ksv and Osd are low-K dacite to andesite (SiO2=55.6-64.8wt%, K2O=0.21-0.97wt%, and SiO2=60.7-66.2wt%, K2O=0.08-0.97wt%, respectively). Kav shows low-K andesitic compositions (57.4-57.6wt% in SiO2, 0.42-0.43wt% in K2O). SiO2 and K2O contents of lava fragments of KfDa are 59.8-63.7wt% and 0.75-1.15wt%, respectively, categorized in low-K~medium-K dacite to andesite. On plots of Harker diagrams in major elements, Ksv forms similar trends to Eruption stage 1 products of KfPD. Compositional field of lavas in KfDa overlaps with those of Eruption stage1 and 2 of KfPD.
As a result, the source of KfPD can be estimated to be the Kashiasahidake Volcano owing to its distribution, lateral thickness change of air fall units and petrological similarity. We could not identify the source edifice of KfDa because there is no amphitheater on the adjacent volcanoes and petrographic

characteristics of them (Ksv, Kav, Osd) are not similar to lava fragments of KfDa.

5. Reference

1)Yamamoto,T.(1999), 2) Yamoto,T.(2006), 3)NEDO (1990), 4)Takashima.I.,Kumaki.M.(2012)
5)Suzuki.T.,Murata.M.(2008), 6)Murata.M.,Suzuki.T.(2011), 7)Ban.M.,Talapka.N.(1995)

Keywords: Kamafusayama pyroclastic deposits, Kamafusayama debris avalanche deposit, Kashiasahidake Volcano

Paleostress analysis of dike swarms of the V2 arc magmatism in the Oman Ophiolite

*Susumu Umino[1], Yuki Kusano[2], Atsushi Yamaji[3]

1. Department of Earth Sciences, Kanazawa University, 2. Geological Survey of Japan, AIST, 3. Division of Earth and Planetary Sciences, Kyoto University

The world largest and best preserved Oman Ophiolite provides the entire geological records of intra-oceanic subduction zone formation and arc evolution. The fast-spread oceanic crust consisting of 98-96 Ma MORB-like basalt (V1) was followed by 96-94 Ma arc volcanism (V2) on a shallow dipping subduction zone, most likely resulted from microplate rotation including the spreading axis [1-9]. The V2 volcanism was dominated by arc tholeiitic rocks and terminated with sporadic activities of low-silica boninite. Through the V2 magmatism, the same source mantle shows progressive depletion by stepwise melt extraction, as shown by the lower Nb/Ta ratios for the younger volcanic rocks (V2 boninite < V2 tholeiite < V1)[7]. The V2 arc tholeiitic and boninitic magmas were successfully modelled as the results of progressive remelting of the V1 residual mantle promoted by the high-T hydrous fluid and sedimentary melt liberated from the metamorphic sole as evidenced by the eHf(t) and Sr-Nd isotopic ratios of the amphibolite and metachert in the sole and clinopyroxene separates from boninites [8,10].

Although volcanic stratigraphy and geochemical evolution of the V2 arc magmatism are well constrained, the V2 magma plumbing system is poorly understood. The lower V2 tholeiitic strata are widely distributed over 200 km, however, the upper boninitic rocks show only limited and sporadic distribution with the largest exposure in the north between wadis Hatta and Ahin, where boninitic and tholeiitic volcanic rocks are intimately associated with hypabyssal and plutonic equivalents, such as dikes, gabbronorite and gabbros. In the north of Wadi Fizh, intense E-W-striking dike swarms that cross cut the N-S-striking V1-stage sheeted dikes are considered to be the feeders of the V2 flows and pyroclastic rocks and have emanated from diorite-gabbro-gabbronorite-ultramafic cumulate complex, which intruded into and replaced the V1-stage layered gabbros, sheeted dikes and lavas. On the other hand, the V2 feeders in the south of Wadi Fizh are N-S to NW-SE dikes and low-angle sheets, the latter of which locally form intense swarms and were hence interpreted as cone sheets [12]. We investigated the distribution, structure and lithology of the E-W-striking dike swarms to understand the paleostress field and genetic relationships between the dike swarms and the V2 extrusive rocks and the plutonic equivalents. The dike swarms strike mostly in two directions of WNW-ESE and E-W, and forms four dense clusters of dikes 3-4 km in width and every 5 km apart N-S. The most intense swarms consist of 100 % sheeted dikes that appear between the lower plutonic bodies and the upper V2 strata. The paleostress analysis [12] of the E-W dike swarms shows that each swarm of dikes is divided into a couple of group of dikes with different paleostress orientations. All these dikes indicate vertical to steeply dipping maximum compressive stress axis and high magmatic pressure exceeding the minimum compressive stress, indicating intrusions along extensional shear fractures oblique to the minimum stress axis, as shown by the coexistence of dikes with two different orientation.

[1] Umino et al. 1990. Malpas et al. (eds.), Ophiolites, Oceanic Crustal Analogues, 375 - 384 [2] Umino et al. 2003. Geochem. Geophys. Geosyst., 8618 [3] Weiler 2000. Marine Geophysical Res., 21, 195 - 210 [4] Ishikawa et al. 2002. Geology, 30, 899-902 [5] Miyashita et al. 2003. Geophys. Geosyst., 8617 [6] Kusano et al. 2012. Geochem. Geophys. Geosyst., 1, 32 –33 [7] Kusano et al. 2014. Geol. Soc. London Spec. Pub., 392, 177-193 [8] Kusano et al. 2017. Chemical Geol., 449, 206 –225 [9] Tsuchiya et al. 2012. Lithos,

156-159, 120 –138 [10] Umino et al. 2016. Japan Earth Planet. Sci. Joint MeetingSIT09-11 [11] Lippard et al. 1986. Geol. Soc. London Memoir, 11 , Blackwell Sci. Pub. [12] Yamaji 2016. Island Arc, 25, 72 - 1157

Keywords: Oman Ophiolite, V2 arc magmatism, dike swarm, paleostress analysis, boninite, subduction initiation

The magmatic processes of the latest eruption of Hakusan Volcano

*Yuzuki Ibaraki[1], Susumu Umino[1]

1. Kanazawa University

Low-frequency earthquakes were observed for the first time in 1999 at 37 km in depth beneath Hakusan Volcano, which has 400 year-long cyclic activities for the last 1300 years. It is very likely that Hakusan Volcano may have started the next active period. It is critical to understand the current status of the magma reservoirs beneath Hakusan Volcano in order to anticipate the possible styles of the forthcoming eruptions. For this purpose, I studied the latest volcanic products in 17th century of Hakusan Volcano to understand the magmatic conditions.
Hakusan Volcano consists of 4 stratovolcanoes. The latest, Younger Hakusan Volcano began its activity at ca 50 ka. A projectile in the south of the summit craters of the latest eruptions was chosen for detailed analysis of the magmatic conditions.
Together with the disequilibirum phenocryst assemblage, phenocrystic hornblende is decomposed and surrounded by clinopyroxene, orthopyroxene. Rims of orthopyroxene phenocrysts show a wide range, while cores show bimodal compositions. The wide and disequilibrium mineral chemistry and textures, combined with incompatible phenocryst assemblage, led us to conclude the mixing origin for the sample with three magmas: basalt magma, andesite magma, and dacite magma. The plagioclase-hornblende thermobarometry (Holland and Blundy, 1994) was applied to a zoned hornblende with plag inclusions showed the increase in T from 800℃ to 950℃ without changing P, and then gradual increase in both T and P to 1000℃ and 0.9 kb. The final T recorded by the groundmass cpx-opx pairs indicates 1250℃. The above T-P path suggests that the dacite magma was initially highly crystalline near the solidus at 800℃ and 7-8 km in depth. The dacite magma was injected by the andesite magma that remelted and remobilized the dacite, both of which were partially mixed together and started to ascend. At a depth of ~2.5 km, the basalt magma was injected into the ascended dacite magma batch and triggered the eruption.

Keywords: Hakusan Volcano, magmatic processes, magma mixing, reverse zoning, geothermometer

Eruption history and magma plumbing system of Akanfuji in the Me-akan volcano, eastern Hokkaido, Japan

*Eiichi Sato[1], Keiji Wada[2]

1. Institute for Promotion of Higher Education, Kobe University, 2. Earth Science Laboratory, Hokkaido University of Education at Asahikawa

Akanfuji, situated in the Me-akan volcano of Eastern Hokkaido, started its eruption ca. 2.1 ka, and its activity continued for 1,100 years. During this period, 17 eruption deposits (Akf-1-Akf-17) can be discerned. The mode of the eruptions of this volcano was mainly of the scoriaceous sub-plinian type. Lava flows are often associated with the scoria eruption. The eruption history of Akanfuji is divided into five stages. In the first stage (Akf-1), scoria fall with many lithic fragments was deposited from northeast to east of the volcano. In the second stage (Akf-2-Akf-3), two larger eruptions occurred and coarse scoria falls were deposited to the northeast. In the third stage (Akf-4-Akf-13), some eruptions occurred and the scoria falls were dispersed in a northeast to southeast direction. This stage is characterized by the finding of orthopyroxene in the deposits. In the forth stage (Akf-14-Akf-16), three larger eruptions occurred and voluminous scoriae were deposited to northeast (Akf-14) and from southeast to south (Akf-15-Akf-16). In the final stage (Akf-17), fine scoria fall was deposited from northeast to southeast. Akanfuji had erupted basalts through its history. Two types of basalts (types I and II) are recognized on the basis of phenocrysts assemblage. Type I is orthopyroxene (opx) bearing olivine (ol)-crynopyroxene (cpx) basalt and Type II is cpx bearing ol-opx basalt. Both types show mineralogical evidences of magma mixing, which are reaction products such as cpx overgrowth around opx phenocrysts, wide range of core compositions, and coexistence of normaly and reversely zoned plagioclase, olivine, and pyroxenes. Zoning profiles of these phenocrysts show timing of magma mixing. We can estimate the time from mixing of the basaltic magmas to the eruption.

Keywords: Me-akan volcano, Akanfuji, Magma mixing

Progress of magma mixing by analysis of heterogeneous fragments from Rawan pyroclastic flow at 9 ka, Me-akan volcano, eastern Hokkaido

*Yuma Endo[1], Keiji Wada[1], Eiichi Sato[2]

1. Earth Science Laboratory, Hokkaido University of Education at Asahikawa, 2. Institute for Promotion of Higher Education, Kobe University

At Me-akan volcano, eastern Hokkaido, pyroclastic activity of plinian fall and pyroclastic flows including pumice and scoria have occurred at 13000-12000 years ago, forming Nakamachineshiri crater with 1.1 km diameter (Wada, 1989). At about 9000 years ago, pyroclastic flow containing pumice, scoria and heterogeneous juvenile ejecta such as banded pumice was flowed down along the Rawan river southwestern of Nakamachineshiri crater. We call this Rawan pyroclastic flow. We analyzed the chemical composition of groundmass glass and plagioclase phenocrysts and groundmass in two specimens of each pumice, scoria and banded pumice in detail.
The groundmass composition of scoria shows SiO_2=61-70wt.% and has fixed chemical trend, whereas that of pumice concentrates to SiO_2=77-79wt.%. The scoria part in the banded pumice varies from SiO_2 =61-76wt.% and shows wide compositional range connecting with scoria and pumice compositions. The pumice part in the banded pumice is slightly higher SiO_2 composition (78-80wt.%) than pumice fragment. Plagioclase phenocryst of scoria and pumice shows almost the same bimodal An content distribution of An58-60 peak and An72-92 wide peak. The lower An plagioclase phenocrysts of both scoria and pumice show the same texture, but the high An plagioclase phenocrysts are different origin between scoria and pumice; rapid crystrallization from mafic magma for scoria and long storage in magma chamber for pumice.
These results suggest that each magma produced scoria or pumice was already mixed in the single or plural magma chamber, and mafic magma produced scoria was injected into felsic magma produced pumice to mingle and mix in the conduit. Diffusion rate of mafic magma is faster than that of felsic magma, mixing proceeds inside of mafic magma incorporating felsic magma in central part in the conduit, producing the banded pumice.

Keywords: Me-akan volcano, magma mixing, banded pumice

Petrology of Takikawa monogenetic volcano group and Shokanbetsu volcano: Temporal and spatial variation of magma at the arc-arc junction

*Ryunosuke Enoeda[1], Mitsuhiro Nakagawa[1]

1. Hokkaido University

Takikawa volcanic field is located at the junction of the Kuril and the northeastern (NE) Japan arc. It consists of Takikawa Monogenetic Volcano group (TMV) and some polygenetic volcanoes: Shokanbetsu volcano group (SHV) and Irumukeppu volcano (IKV). These volcanoes were active during late Miocene to early Pleistocene, and have ceased their activity since 1.7 Ma (Nakagawa et al., 1993). TMV exists in the central area of Takikawa volcanic field, composed of basaltic lava cone, dyke and sill. SHV consists of some polygenetic volcanoes with basaltic-andesitic lava flows in the western area of Takikawa volcanic field. IKV, located in the eastern area of Takikawa volcanic field, is a polygenetic volcano, consisting of andesitic lava flow. There are several previous studies about volcanic rocks in this district (Oba, 1972; Yagi et al., 1987; Nakagawa et al., 1993; Okamura et al., 2000). Although several major and trace elements about TMV and SHV are reported, the comprehensive petrological and geochemical features of the volcanic rocks from Takikawa volcanic field have not been still revealed.
Monogenetic volcanoes at this district could have been formed under extensional stress field accompanied with spreading of Takikawa structural basin (Nakagawa et al.,1993). Therefore, the geochemical features of Takikawa volcanic rocks are expected to reflect temporal and spatial variations of magmatism around the junction of the Kuril and the NE Japan arcs during late Miocene to early Pleistocene. These features can provide us the important constraint for understanding the tectonics at the arc-arc junction. In order to reveal the magmatic process at arc-arc junction, we have been carried out the petrological and geochemical study about Takikawa volcanic field. We investigated 17 rock bodies in TMV, three volcanoes of SHV: Minamishokan, Etai and Ofuyu. In this presentation, we report the petrographical features, and major and trace elements of whole-rock chemistry of these volcanic rocks.
Most of rocks in TMV are augite-olivine basalt. They are absent from plagioclase.. Andesite including plagioclase, hypersthene, and resorbed quartz are rarely occurred. In Minamishokan, the rocks in upper part are hypersthenes-augite andesite with plagioclase and mafic inclusion. In contrast, the lower rocks are quartz-bearing olivine basalt, including plagioclase with dusty zone and resorbed quartz with augite reaction rim. The rocks of Etai are clinopyroxene-olivine basalt, having plagioclase with dusty zone and inclusions with glomeroporphyritic texture. Ofuyu is composed of quartz-bearing augite-olivine basalt, similar to those of Etai, except for the existence of resorbed quartz.
Focusing on incompatible elements of the primitive basalt, SHV has relatively narrow range showing relatively higher Rb/Zr and Ba/Zr ratios, and lower Nb/Zr ratio. In contrast, TMV shows relatively wide range with lower Rb/Zr and Ba/Zr ratios, higher Nb/Zr ratio. The various ratios of incompatible elements of primitive basalts in this district cannot be produced by crystallization of a single primary magma, but be derived from multiple various primary magmas. Considering the difference in ratios of incompatible elements primitive basalts, SHV has the feature of island arc basalt (low-Nb/Zr and high-Ba/Zr ratios). TMV exhibits the feature of back arc basin basalt with.high-Nb/Zr and low-Ba/Zr ratios. These spatial distribution of ratios of incompatible elements shows ellipse zonation, similar to the zonation of SiO_2 wt.% reported by Nakagawa et al. (1993). This feature might reflect the difference in degree of partial melting at producing primary magma or the compositional variation in mantle source, corresponding to the mantle plume model under this district, of which SHV as a center, proposed by Nakagawa et al. (1993). In

order to examine this possibility, we are going to carry out the additional geochemical study using rare earth elements and isotopic compositions.

Keywords: Monogenetic volcano group, Shokanbetsu volcano, Arc-arc junction, Basalt, Mantle plume

Formation history and active age of Iwaonupuri Volcano of Niseko volcanic group,southwestern Hokkaido,Japan

*Ryoko Matsuo[1], Mitsuhiro Nakagawa[1]

1. Hokkaido University

Niseko volcanic group (NVG), located at the northern part of southwestern Hokkaido, is Quaternary volcanoes composed of stratovolcanoes and lava domes. There are some previous geological studies about NVG (Hirokawa and Murayama, 1955; Oba, 1960; NEDO, 1986, 1987). It is revealed that NVG started its activity at 1.6 Ma and the active area had moved from west to east. It is believed that Iwaonupuri volcano is the youngest volcano in NVG on the basis of the fresh morphology as well as fumarolic activity. Okuno (2003) reported the ^{14}C age from the soil beneath Iwaonupruri tephra: ca.6 ka. However, he also indicated the low reliability of this ^{14}C age, and the source and eruption style of this tephra are still unclear. Therefore, in order to reveal the eruptive history and eruption style of the NVG, especially in Holocene epoch, we performed geological study about NVG.
Iwaonupuri and Nitonupuri have been considered as the youngest volcanoes in NVG. The rocks of both volcanoes are andesite, containing plagioclase, clinopyroxene, orthopyroxene, and magnetite phenocrysts. In addition, the rocks of Nitonupuri have hornblende. On whole-rock chemistry, Iwaonupuri can be clearly distinguished from Nitonupuri on many Harker diagram. According to vent location, stratigraphical relationships, petrological features, it is considered that these two volcanoes are the distinct ones. Therefore, we define the volcano has been active after the activity of Nitonupuri as Iwaonupuri, which is the youngest one in NVG.
Iwaonupuri (1,116 m a.s.l.) is located at the eastern part of NVG. This volcano has been built on the east of Nitonupuri, composed of a pyroclastic cone and several lava domes and lava flows. Iwaonupuri Big Crater pyroclastic cone (IBC) with a crater (ca. 1km in diameter) locates at the western part of Iwaonupuri. Sho-Iwaonupuri lava dome (SI) exists in this crater. IBC and SI are covered with the Dai-Iwaonupuri volcanic edifice (DI). DI consists of the lower lava dome and the upper lava flows distributed from the summit to the east. In addition, several small craters such as Gosikionsen crater are found in the whole area of Iwaonupuri. Iwaonupuri volcano can be divided into five units on the basis of stratigraphic relationship, eruption style and the location of the eruptive center: IBC pyroclastic rocks, SI lava dome, DI lower lava dome, DI upper lava flows, and Iwaonuouri phreatic explosion breccia in ascending order.
The activity of Iwaonupuri started with forming IBC. At first, phreatic eruptions occurred. After that, its activity changed to the magmatic eruptions, forming eruption column and generation pyroclastic flows intermittently. This activity provided Nsiw-1 tephra found by Okuno (2003). The thickness as well as the grain size of component in this tephra become larger from east to west, suggesting that this tephra can be correlate with IBC. In this study, we obtained two ^{14}C ages: 9480 cal.yBP from the charcoal in the pyroclastic flow and 10910 cal. yBP from the soil beneath the Nsiw-1 tephra. Accordingly, it is concluded that Iwaonupuri started its eruptive activity about 9,500 years ago and has extruded lava domes and lava flows repeatedly. It is also considered that phreatic and phreatomagmatic eruptions were occurred contemporaneously, to form many explosion craters in the whole area. Although the latest magmatic eruption is DI upper lava flows from the summit, the phreatic eruptive activity would have continued after this eruption. Actually, we obtained “Modern” as the result of the ^{14}C age from a layer of explosion breccia near Gosikionsen spa. In this study, we revealed the age of the initial stage of Iwaonupuri eruptive activity. Considering the eruption age at 9,500 years ago, the growth history of volcano and the existence of many young explosion craters, it is probable that Iwaonupuri is the volcano with high level of activity through Holocene epoch.

Keywords: Iwaonupuri, formation history, active volcanoes, geology, radiocarbon dating, Niseko volcanic group

Reexamination of late Pleistocene tephras of Shikotsu-Toya Volcanic Field

*Mizuho Amma-Miyasaka[1], Mitsuhiro Nakagawa[1], Daisuke MIURA[2], Shimpei Uesawa[2], Ryuta FURUKAWA[3], Akiko Matsumoto[1]

1. Hokkaido University, 2. Central Research Institute of Electric Power Industry, 3. Advanced Industrial Science and Technology

Shikotsu-Toya volcanic field (STVF) in southwestern Hokkaido is located at an arc-arc junction of Kuril and NE Japan arcs, and composed of three caldera volcanoes (Shikotsu, Toya and Kuttara) and Yotei & Shiribetsu stratovolcanoes. Advanced tephrochronological studies have been undertaken to establish the sequence of the pyroclastic flow and pyroclastic fall deposits in STVF (Kasugai et al., 1980; Yamagata, 1994; Machida, 1999). Combined with precise AMS ^{14}C dating and Marine Oxygen Isotope Stage (MIS) determinations, explosive eruptions have been repeated during 130-40 ka (Yamagata, 1994; Katoh et al., 1995; Machida and Arai, 2003; Sase et al., 2004). However, stratigraphy of these tephras has not been revised since 1990's and identification of tephra layers was mainly based on petrography and refractive index of glasses for the caldera volcanoes. Furthermore, it is suggested that Yotei and adjacent Shiribetsu volcanoes has erupted since ca. 50 ka (Nakagawa et al., 2011; Uesawa et al., 2016).
In this study, geological survey has been done mainly in southern and eastern part of lake Shikotsu (< 65 km). Pyroclastic flow deposits of Shikotsu caldera-forming eruption widely and thickly covered around the lake, we also carried out boring explorations in the proximal area (10 km and 25 km east from the lake center), and observed two cores of Japan Meteorological Agency (10 km south) and National Research Institute for Earth Science and Disaster Prevention (25 km SSE). We used four thick tephra layers as key beds in STVF; Spfa-1 & Spfl, Kt-1, Ssfa & Ssfl and Toya. To correlate tephra layers, we firstly investigate stratigraphic relationships with key tephra layers and then compare petrological characteristics with proximal samples. Then, we distinguished at least 27 tephra layers in STVF, and discovered six new tephra layers in this study. As a results, the beginning of eruptive activity dates back to 120 ka for Shiribetsu volcano and ca. 80 ka for Yotei and Shikotsu volcanoes.
Together with K-Ar ages of volcanic rocks around this area, eruptive history of STVF are summarized as follows. Andesite volcanism had occurred until middle Pleistocene and had terminated around 0.6-0.5 Ma. After a long dormancy (ca. 400 ky), STVF started its eruptive activity 130 ka at Toya, and 120 ka at Yotei volcanoes. A catastrophic caldera-forming eruption occurred ca. 110 ka at Toya volcano. Then, the activity has propagated toward the east. Kuttara and Shikotsu volcanoes started their activity almost simultaneously ca. 90 and 85 ka, respectively. Subsequently, a large stratovolcano; Yotei has been also constructed since ca. 75 ka at the back-arc side of the STVF. The explosive eruptions of VEI=5-6 had repeated at Kuttara and Shikotsu volcanoes, and VEI=6 eruption occurred at Kuttara, and the largest caldera-forming eruption in the STVF occurred at Shikotsu volcano (VEI=7) ca. 45 ka. Since then, Yotei and post-caldera volcanoes in STVF have continued their eruptive activity until now. It should be noted that there exist three active periods during 130-110 ka, 95-75 ka and 60-45 ka in STVF.

Keywords: tephras, late Pleistocene, Shikotsu-Toya Volcanic Field, glass composition

Eruption history of pre-Goshikidake, Zao volcano

*Yuki Nishi[1], Masao Ban[2], Oikawa Teruki[3]

1. Graduate School of Science and Technology, Yamagata University, 2. Department of Earth and Enviromental Science, Faculty of Science, 3. Advanced Industrial Science and Technology

Introduction

Zao volcano is an active stratovolcano in NE Japan, and has a long-eruption history of ca. 1 million years. At the beginning of the newest stage (ca. 35 ka to present), horseshoe shaped Umanose caldera was formed in the summit area. The Goshikidake, the youngest cone, has grown up in the caldera from ca. 2 ka and now its relative elevation are about 110m and bottom diameter is about 850m. The present crater lake Okama is in the western part of the Goshikidake and its diameter about 360 m. The Okama has been active since ca. 0.8 ka and the pre-crater was southeast ward of the Okama. Former studies showed that the cycles from phrenetic to phreatomagmatic eruptions repeatedly occurred, delimited by dormant time. We examined the eruption history during ca. 2 to 0.8 ka based on near vent facies features.

Pre Okama-Goshikidake

Previous study subdivided Goshikidake pyroclastic rocks into 5 units by angular unconformities. Unit 1, 2, 3 were formed during ca 2 ~ 0.8 ka. We define an edifice composed of unit 1~3 products as the pre-Goshikidake. The unit 1~3 products are well exposed in the southern part of the Goshikidake. Our study is based on observation of the products exposed in this area.

unit1

The maximum total thickness of unit 1 is about 20 m. Based on the lithofacies, we subdivided unit 1 products into 7 layers. Layer 1 and 2 are composed of lapilli-tuff. The matrix is hydrothermally altered clay. Layer 1 and 2 are different in color. Layer 3, 5, 7 are composed of strongly stratified thin layers of tuff to lapilli-tuff, showing various kinds of lamination and sagging. Matrix color is gray in layer 3, and raddish brown layer 5 and 7. Layer 4 and 6 are composed of tuff-breccia, including reddish ~ gray colored scoria.

unit2

The maximum total thickness of unit 2 is about 20 m. These products are subdivided into 4 layers. Layer 1, 4 are composed of strongly stratified thin layers of tuff to lapilli-tuff, showing various kinds of lamination and sagging. The matrix is gray to red-radish ash and scoriaceous bombs and volvcanic blocks concenrated parts are sometimes observed. Layer 2 is composed of agglomerate with various amounts of volcanic bombs and scoria. Layer 3 is composed of strongly laminated tuff, its lower is gray and upper is red in color.

unit3

The maximum total thickness of unit 3 is about 20 m. These products are subdivided into 7 layers. Layer 1, 3, 5 are composed of gray colored tuff, and change in quality with small scoria little bit. Layer 2, 4 are composed of strongly stratified thin layers of tuff to lapilli-tuff, showing various kinds of lamination and sagging. The matrix is radish~red-radish ash and scoriaceous bombs and volvcanic blocks concenrated parts are sometimes observed. Layer 7 include both facies. Layer 6 is scoria fall deposit with ~2 m scoria in the scoriaceous matrix. This is observed in southeast and gets thin rapidly to southwest.

The eruption sequence of pre-Goshikidake

Based on these observations, layer 1, 2, 3 of unit 1, layer 3 of unit 2, layer 1, 3, 5 of unit 3 would be by phrenetic eruption products, while layer 4, 5, 6, 7 of unit 1, layer 1, 4 of unit 2, layer 2, 4 of unit 3 would be formed by the phreatomagmatic eruption. Layer 7 of unit 3 include both types. The layer 2 of unit 2 would be vulcanian type like eruption, layer 6 of unit 3 would be scoria fall products.

In the unit 1, the activity began by phrenetic eruptions and changed to phreatomagmatic eruptions. The

unit 2 activity is characterized by repeat of phreatomagmatic eruptions. In the middle part, vulcanian type like and phrenetic eruptions would occur. In the unit 3, the cycle of phrenetic to phreatomagmatic eruptions repeated several times. The strombolian type eruption additionally occurred in the climax.

The migration of the crater location

The crater of unit 1 would be located slightly eastward of pre-crater, based on strike and dip data of unit 1 products. The unit 2 and 3 products were erupted from the pre-crater, revealed by tracking the unit 2 and 3 layers to the eruption center ward. Considering the present crater is in west ward of the pre-crater, the crater migrated stepwise from east to west past ca. 2 ky.

Keywords: Zao volcano, Goshikidake, Eruption history, Pyroclastic surge

Glaciovolcanic and magmatic evolution of Ruapehu volcano, New Zealand

*Chris Conway[1], Colin Wilson[2], John Gamble[2], Graham Leonard[3], Dougal Townsend[3]

1. National Museum of Nature and Science, 2. Victoria University of Wellington, 3. GNS Science

Chronostratigraphic studies of continental arc stratovolcanoes reveal the timing and types of past eruptive behaviour and are therefore crucial for constraining magma evolution models as well as the future eruption potential in these active settings. Such studies can be complicated by complex stratigraphic relationships caused by glaciovolcanism (eruptions in the presence of ice), glacial erosion and sector collapse for edifices that have been glaciated. These issues are relevant to the numerous high-altitude cones that define Earth's continental volcanic arcs. A key example of this is Ruapehu, which is an active andesite-dacite stratovolcano located at the southern end of the Taupo Volcanic Zone, New Zealand. The growth of the Ruapehu edifice has occurred throughout coeval eruptive and glacial histories since ~200 ka. Here, new high-precision $^{40}Ar/^{39}Ar$ ages and whole-rock major and trace element data for Ruapehu lava flows are integrated with geological mapping and glacier reconstructions. The data provide a high-resolution chronostratigraphic and geochemical framework for investigating processes of ice-marginal lava flow emplacement and magma generation. In particular, the following concepts are addressed in this study: (1) the potential for ice-bounded lava flows to provide paleoclimate information; (2) the role of deglaciation in triggering Holocene sector collapses; (3) the variable extent of crustal assimilation in andesite-dacite magma genesis during the lifetime of a stratovolcano.

Keywords: lava-ice interaction, andesite petrogenesis, Ruapehu volcano

Formation process of plagioclase aggregates of the 1991-1995 eruption at Unzen

*Yuriko Konishi[1], Atsushi Toramaru[2]

1. Department of Earth and Planetary Science, Graduate School of Science, Kyushu University, 2. Department of Earth and Planetary Sciences, Faculty of Sciences, Kyushu University

We conduct the petrographical description, the textual analysis including crystal size distribution (CSD) analyses and chemical analyses for plagioclase phenocrysts which show frequently the aggregate texture in volcanic rocks of the eruption. In this study, to know the basic information before discussing the magmatic system of the 1991-1995 eruption at Unzen, we focus on plagioclase aggregates and their formation process. Plagioclase phenocrysts can be classified into two types on the basis of textural observation using optical microscopes. Type S phenocrysts exist as a Solo crystal without forming aggregates. Type A phenocrysts have the Aggregate texture in which a phenocryst recognized in hand specimen consists of two to several single crystals. The dusty zone can be found in both types. We conduct CSD analyses for type S, type A and component crystals of type A (type A_{comp}). We conduct chemical analyses for cores and rims of type S and type A_{comp}. Results from CSD analyses show that CSD plots of all types follow the exponential distributions. It is remarkable that CSD plots of type S have steeper slopes and smaller maximum crystal sizes than those of type A_{comp} have. Results from chemical analyses also show the difference in core Anorthite (An) contents; type S has broader range (around An 35-60) than type A_{comp} has (around An 40-55). These results suggest the difference in a magmatic system where each type of plagioclase phenocrysts has crystallized. We propose two models that can explain the characteristics of CSD plots and core An content of the plagioclase phenocrysts; the coalescence model and the separation model. Assuming the coalescence model, we suggest that nucleation rate has increased at a certain time and aggregations have occurred at a certain time interval. On the other hand, assuming the separation model, we suggest that the injection of a high-temperature mafic magma including high-An solo crystals has melted country rocks including plagioclase with core An 40-55. We also suggest that fragments separated from country rocks have assimilated with the mafic magma. Because the slight differences in the CSD trends and the compositional ranges between type S and A_{comp}, which has been detected in this preliminary analysis, may be an important clue to discriminate which process is realistic, we will have to conduct more comprehensive and detail analysis including correlations between size and compositions, trace element compositions, etc.

Keywords: Crystal size distribution, Plagioclase, Aggregate, Mt. Unzen

Modeling the chemical evolution of open-system magma chambers using the principles of heat and mass transfer and thermodynamics

*Koshi Nishimura[1]

1. Toyo Univ.

A model of the chemical evolution of open-system magma chambers has been developed using the principles of heat and mass transfer, and thermodynamics. Generally speaking, thermal Rayleigh numbers for high-temperature, crystal-poor magma chambers are very large, resulting in vigorous thermal convection (Martin et al., 1987). However, convection is suppressed following ~50% crystallization because of the formation of an interlocking framework of crystals. This study focuses on the earlier convection stage of sheet-like magma chambers, prior to significant crystallization.
The model incorporates the effects of concurrent magma influx (recharge or mixing), roof-rock assimilation, magma extraction, and fractional crystallization. Magma influx affects magma composition and temperature, while the rate of roof-rock assimilation is controlled by convective heat flux from the magma and the effective fusion temperature of the roof rock (Huppert and Sparks, 1988; Koyaguchi and Kaneko, 1999). Crystal settling occurs at the floor of the magma chamber (Martin and Nokes, 1988). Equilibrium phase relations and the partitioning of major elements between mineral phases and coexisting liquid are calculated thermodynamically using the rhyolite-MELTS algorithm (Gualda et al., 2012). Trace element and isotopic variations of the magma are calculated using open-system chemical mass balance equations (Nishimura, 2012).
The model quantifies the evolution paths of major and trace elements, and isotopes within crystals, liquid, magma, and crystal rims. Of note, it also shows that the rate of magma influx strongly affects crystal core-to-rim profiles of trace-element concentrations and isotopic ratios.

Keywords: magma chamber, geochemical model, heat and mass transfer

Magmatic plumbing system of a complex ocean island volcano, Ascension Island, south Atlantic

*Katy Jane Chamberlain[1], Katie Preece[2], Jenni Barclay[3], Jane H Scarrow[3,4], Richard J Brown[5], Jon P Davidson[5], Darren Mark[2]

1. Japan Agency for Marine-Earth Science and Technology, 2. SUERC, East Kilbride, UK, 3. University of East Anglia, Norwich, UK, 4. University of Granada, Granada, Spain, 5. Durham University, Durham, UK

Ascension Island, 7˚56’ S, is an isolated composite volcano in the south Atlantic, lying 90km west of the Mid Atlantic Ridge. Even though Ascension Island is small –only 12 km in subaerial diameter –it has produced a wide variety of eruptive products in its 1-million-year subaerial eruptive history. Volcanic rock compositions range from basalt to rhyolite, following a silica-undersaturated subalkaline evolutionary trend. Yet, while a huge variation in magmatic compositions have been erupted across a limited spatial extent, there is little evidence for magma mixing preserved in erupted deposits.

Here we present extensive whole rock XRF data coupled with EPMA and LA-ICPMS analyses of glass and crystals of samples which span the entire range in compositions erupted throughout Ascension Island’s subaerial history. These new geochemical data are coupled with detailed field observations and targeted $^{40}Ar/^{39}Ar$ dating, which reveal more than 70 explosive pumice-producing eruptions, and more than 40 mafic effusive eruptions have occurred in the last 1-million years. We use these data to construct a robust volcanic history for Ascension Island, including dating its most recent activity, and build a detailed petrological model for the magmatic plumbing system underlying Ascension. These data highlight the role of fractional crystallisation in the production of the range of magmatic compositions found on Ascension Island, and reveals the closed-system nature of the magmatic plumbing system, unlike many other ocean islands, such as Tenerife or Iceland. SIMS-measurements of volatiles in melt inclusions in two zoned fall deposits appear to show this closed-system evolution occurs at depths between 7 and 11 km, i.e. the lower crust. The closed-system and relatively deep nature of magmatic evolution, and the relatively small volumes erupted in single events means that any explosive future activity is unlikely to preceded by significant precursory signals.

Keywords: Ocean Island Volcanism, Magmatic evolution, Crustal Structure

Raman spectroscopy applied to reveal the oxidation state of the “Red” obsidian from Shirataki, Hokkaido, Japan

*Kyohei Sano[1], Eiichi Sato[2], Keiji Wada[3]

1. Shirataki-Geopark, 2. Kobe University Institute for Promotion of Higher Education, 3. Hokkaido University of Education at Asahikawa

Silicic volcanism ranges from explosive to effusive. Understanding what controls in such activity is an important issue to explain the explosive-effusive transition. The recent observation on Cordon Caulle (Chile, 2011–12) revealed that explosive-effusive hybrid activity (Schipper et al., 2013) and the oxidation state in volcanic products have attracted attention to reveal the effusive-explosive transition during magma ascent, especially on viscous magma eruptions (e.g. Castro et al., 2014). The Laser Raman spectroscopy is expected to give information about micro-scale oxidation state based on the specification of oxide microlite and glass amorphous structure in volcanic rocks.
At the Akaishiyama obsidian lava on Shirataki, northern Hokkaido, Japan, we can observe the red-colored oxidized obsidian mingled with black-colored obsidian. The mingled shows various contrasts and distributions on the hand specimen, and we can consider that such a various oxidation texture reflect the different mechanisms of outgassing process during the eruption. In this study, we used the microRaman spectroscopy to characterize the oxidation state in the obsidian, using a JASCO NRS-7100 Laser Raman Spectrometer with 514 nm excitation at Kobe University Research Facility Center for Science and Technology, Japan. We obtained the 2 types of Raman spectra of oxide microlites in red and black obsidians, respectively. Compared with referential spectra, we identified captured spectrum as magnetite and hematite. Based on the analytical results of microRaman Spectrometer and distribution pattern of oxidation texture, we can discuss the formation process of heterogeneous oxidation textures during the eruption.

Keywords: obsidian, Raman spectroscopy, textural analysis, Shirataki

Petrographic description and density analysis of fall deposit by the May 18, 1980, eruption of Mount St. Helens.

*Haruka Ino[1], Atsushi Toramaru[2]

1. Department of Earth and Planetary Sciences, Graduate School of Sciences, Kyushu University, 2. Department of Earth and Planetary Sciences, Faculty of Sciences, Kyushu University

The May 18, 1980, eruption of Mount St. Helens, Washington, erupted white pumices that have the same composition from 08:32 to 18:15 LT. Characteristics of eruption of Mount St. Helens are represented by the dramatic land slide and subsequent plinian eruptions. Phenocrysts and pheno-bubble textures of fall deposits record state in the conduit just before the plinian eruptions. In this study, correlations between texture of fall deposit and time evolution of eruption are examined. Samples of this study were taken from fall deposits divided into seven layers with 2 cm in thickness. The uppermost layer is referred to as layer 1, layers below are identified by following sequential integers. Measurement of bulk density and description of texture were carried out for white pumices with 8~16mm in radius in each layer. Bulk density was calculated on the basis of bulk volume by 3D image. Thin sections were made for white pumices with the average in mass, bulk volume and bulk density in each layer and the maximum and minimum bulk density in layer 1. Measured bulk density ranges 0.495~1.01g/cm³. Statistical made of bulk density is 0.7~0.8g/cm³in the intermediate bin for layer 1 and 2, whereas that is in the smallest bin 0.5~0.6g/cm³ and the abundance of pumices monotonically decrease with bulk density for layer 3 and 4. Layers 1 and 2, as well as layers 3 and 4 resemble in bulk density distribution and petrographic texture. Specifically in the petrographic texture, there are more phenol-bubbles for layer 3 and 4. The maximum and minimum bulk densities in layer 3 are 0.888g/cm³ and 0.505g/cm³, respectively. From backscattered electron images, pumices samples with minimum density include more coalesced bubble than those with maximum one. If we assume the inverse relationship between eruption intensity and pumice bulk density, we can suggest that pumices with the smallest bulk density in layer 4 may be eruption products when the plinian column grew up to the maximum height. We should confirm the trend in texture of pumices by more detail analysis for sufficient numbers of pumices samples with different bulk densities in each layer including bubble size distribution measurement and chemical analysis microlites. Furthermore, from BSD data we should calculate the average bubble nucleation rate and growth rate to infer how bubbles were formed, in addition to the estimation of buoyancy state of the conduit prior to eruptions by pheno-bubble abundance.

Keywords: vesicularity, plinian eruption, density, pheno-bubble

Textural analysis of Blast deposits from the May 18, 1980, eruption of Mount St. Helens

*Mizuki Takehara[1], Atsushi Toramaru[2]

1. Department of Earth and Planetary Sciences, Graduate School of Sciences, Kyushu University, 2. Department of Earth and Planetary Sciences, Faculty of Sciences, Kyushu University

On 18 May 1980 at 08:32 LT, the northern flank of Mount St. Helens (in southern Washington State, USA) collapsed by an M5 earthquake. The landslide caused a giant lateral “Blast” originating from cryptodome. Hoblitt and Harmon (1993) reported two juvenile rock types - gray dacite and black dacite - that are derived from the same cryptodome magma. They are different in bulk density, but their textures have not been analyzed in details. In the present study, therefore, we carry out the textural analysis of two cryptodome dacite - gray dacite and black dacite -, and discuss processes that may have generated two different types of products.

Samples were taken from five layers of deposits at two sites –STOP 6 and STOP 7-. STOP 7 is 45° clockwise from north about 5 km from the vent. STOP 6 is 70° clockwise from north about 10 km from the vent. Samples from three layers, “upper”, “middle”, and “lower” were taken at STOP 6. Samples from two layers “upper” and “lower” were taken at STOP 7. We made a following analysis. (1) Grain size analysis, (2) Component analysis (8-16 mm), (3) Bulk density (8-16 mm), (4) Texture analysis (void and crystal). In analysis of grain size distribution, we sieved the five samples by $2^{-\phi}$ mm metal mesh sieve (ϕ = 2, 1, 0, -1,-2, -3 -4 -5). As the result, it is found that the average grain size of STOP 6 is larger than STOP 7. On the basis of color and vesicularity of grains, we classified each 8-16mm samples into four types (“gray dacite”, “black dacite” “lithic”, and “others”). As the result, it is found that gray dacite and black dacite occupy 70-80 % in volume at each layer. Also, deposit at STOP 7 include more black dacite than at STOP 6. We measured bulk volume of all particles of gray and black dacites with 8-16 mm at each sites by the 3D scanner, and calculated bulk density. As the result, the density of juvenile dacites shows clear bimodal distribution, with peaks at 1.9 gcm^{-3} (gray dacite) and 2.3 gcm^{-3} (black dacite). We observed the texture (void and crystal) of 8-16 mm gray and black dacite particles that represent each layer by reflection microscope and SEM. As the result, although both of them has microlites (small crystals of 1 μ-30 μm) in groundmass, they have quite different textural characteristics as follows: Gray dacites show uniform distribution of rounded vesicles with various sizes (1 μ-200 μm) whereas black dacites show remarkable heterogeneity in vesicle abundance and morphology, that is void-free regions and void-rich regions consisting of angular voids (0.1-1 mm) surrounded by microlites. In addition, in black dacites cracks develop connecting the void-rich regions regardless of presence of phenocryst and groundmass.

From results of the textural study, we speculate that gray dacites had experienced decompression vesiculation, whereas, black dacites had experienced vesiculation by cooling crystallization before the sadden decompression. We suggest that, a first rising magmas corresponding to black dacites had been cooled and crystallization-induced vesiculation at the location close to the surface, and a magmas beneath the cooled magma in cryptodome, corresponding to gray dacites, had preserved relatively large amount of volatile component. Thus, the landslide made cracks in the black dacite magmas by brittle fracturing and bubbles in the gray dacite magmas by vesiculation. Such differences in volatile contents and history in vesiculation and crystallization result in the textural difference revealed by this study.

Keywords: Mount St. Helens, cryptodome, blast

